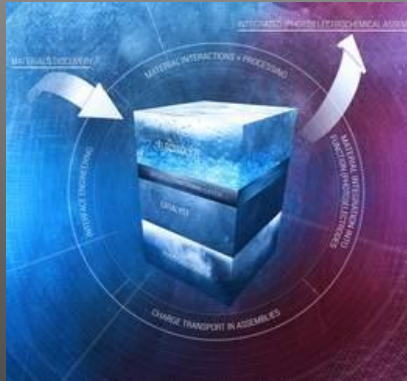
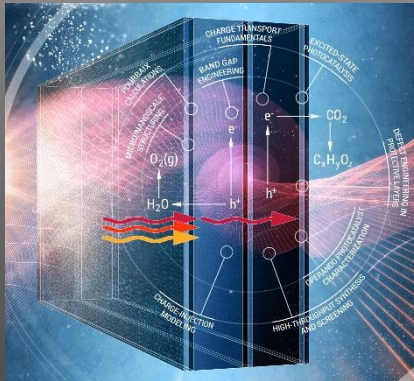
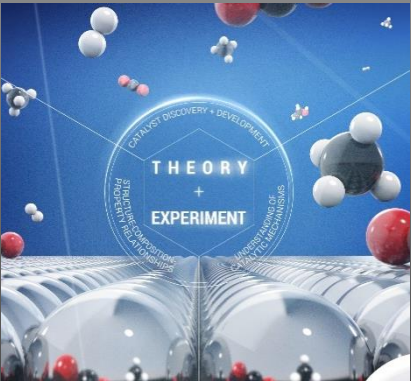


# ARTIFICIAL PHOTOSYNTHESIS—THE SELECTIVE CO<sub>2</sub> REDUCTION CHALLENGE



HARRY ATWATER

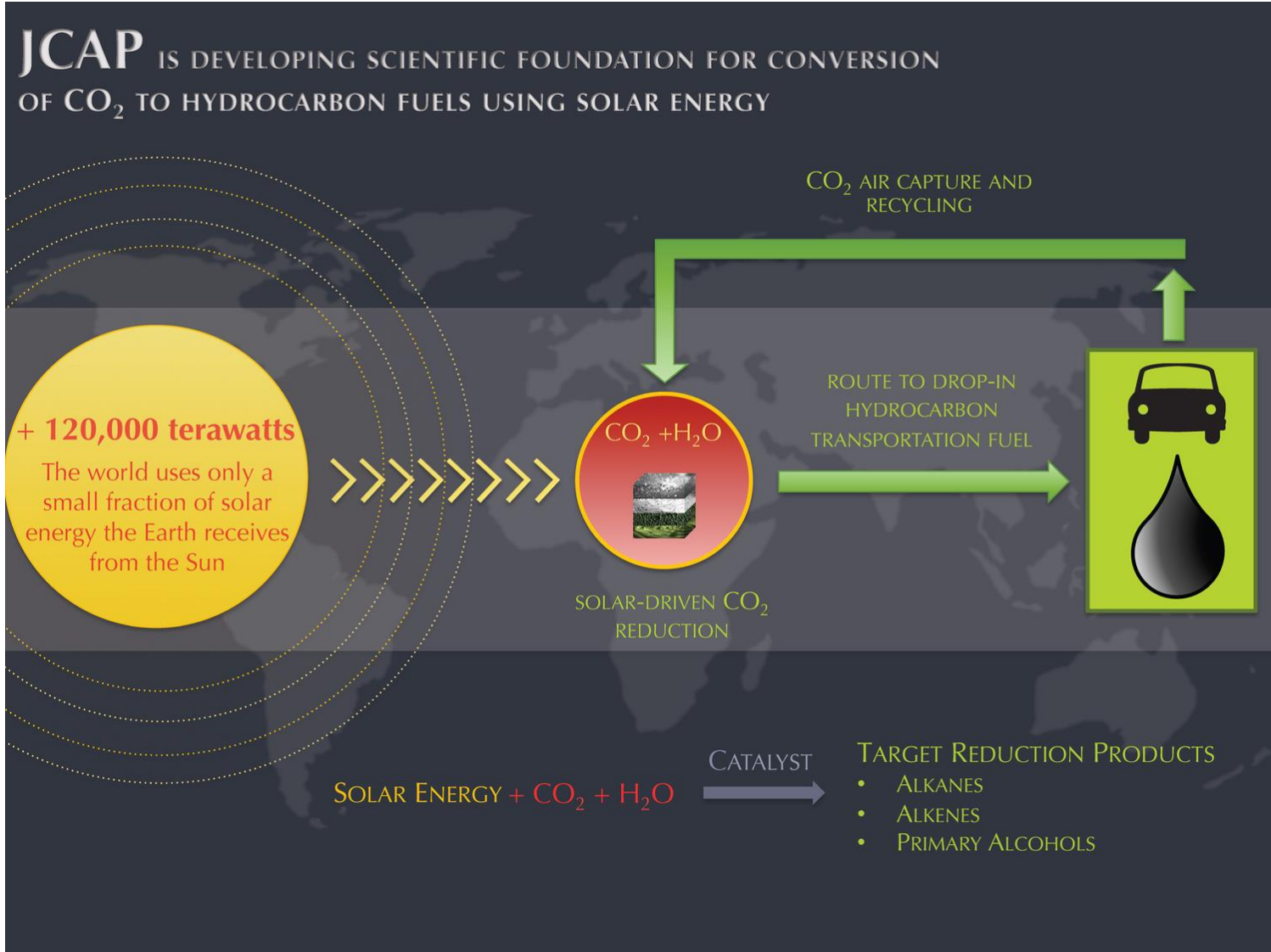
JOINT CENTER FOR ARTIFICIAL PHOTOSYNTHESIS  
ISF-2

July 8<sup>th</sup> 2017



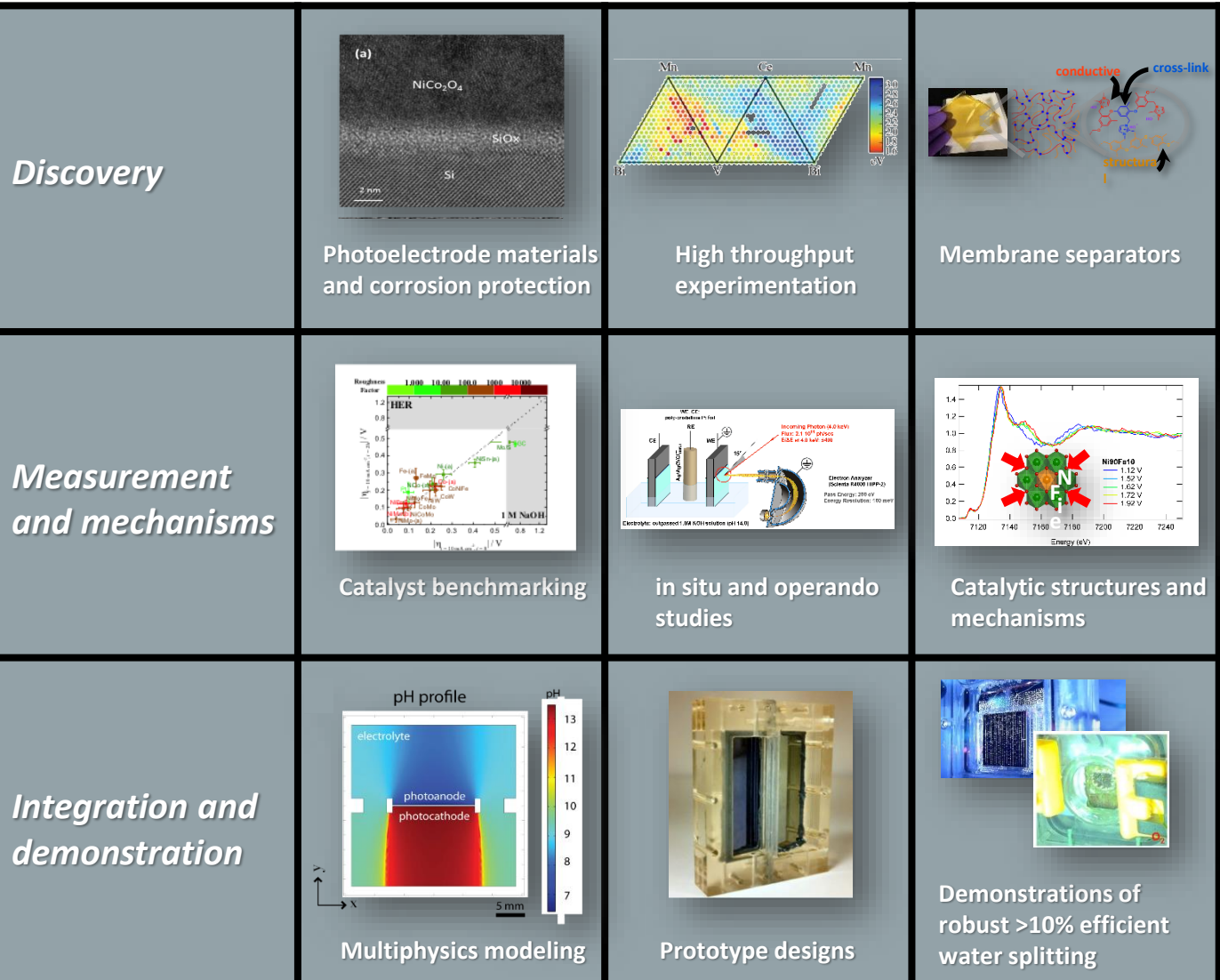
**SLAC**





## JCAP'S FIRST PHASE: SOLAR FUELS FOR WATER-SPLITTING

## Materials



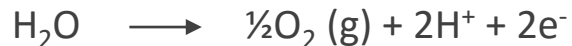
## Devices

# JCAP: SOLAR FUELS GENERATORS

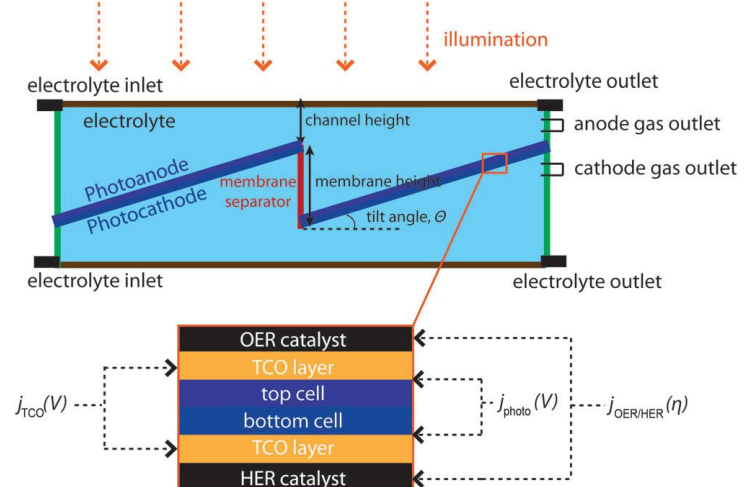
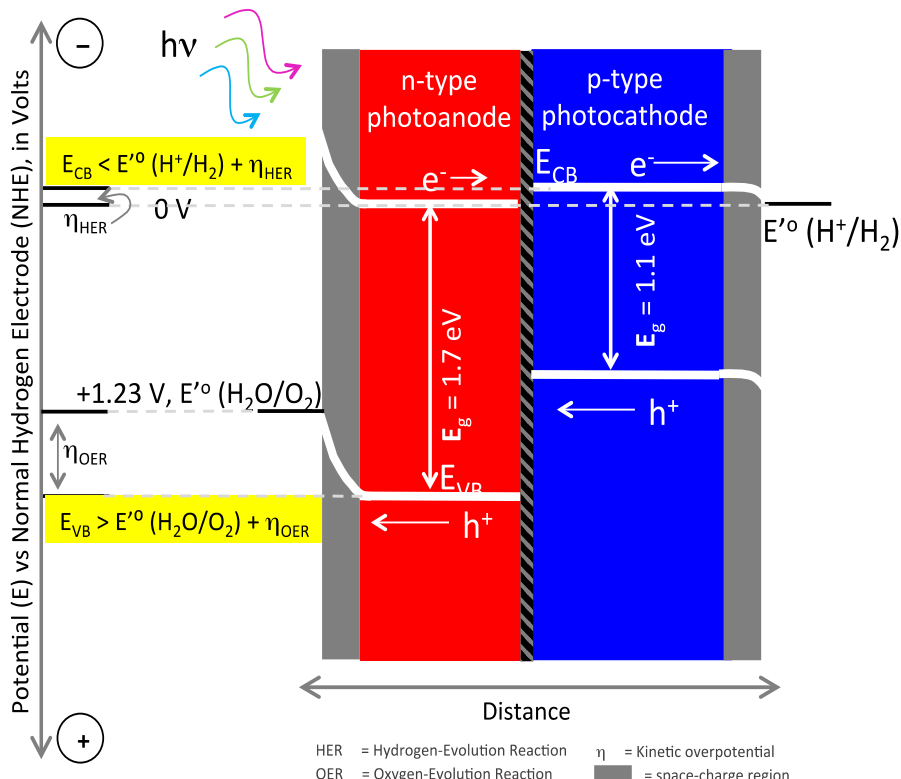
## Hydrogen evolution reaction (HER)



## Oxygen evolution reaction (OER)



## CO<sub>2</sub> reduction reaction (CO<sub>2</sub>RR)

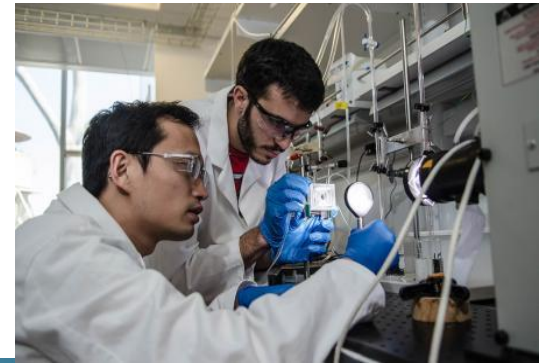
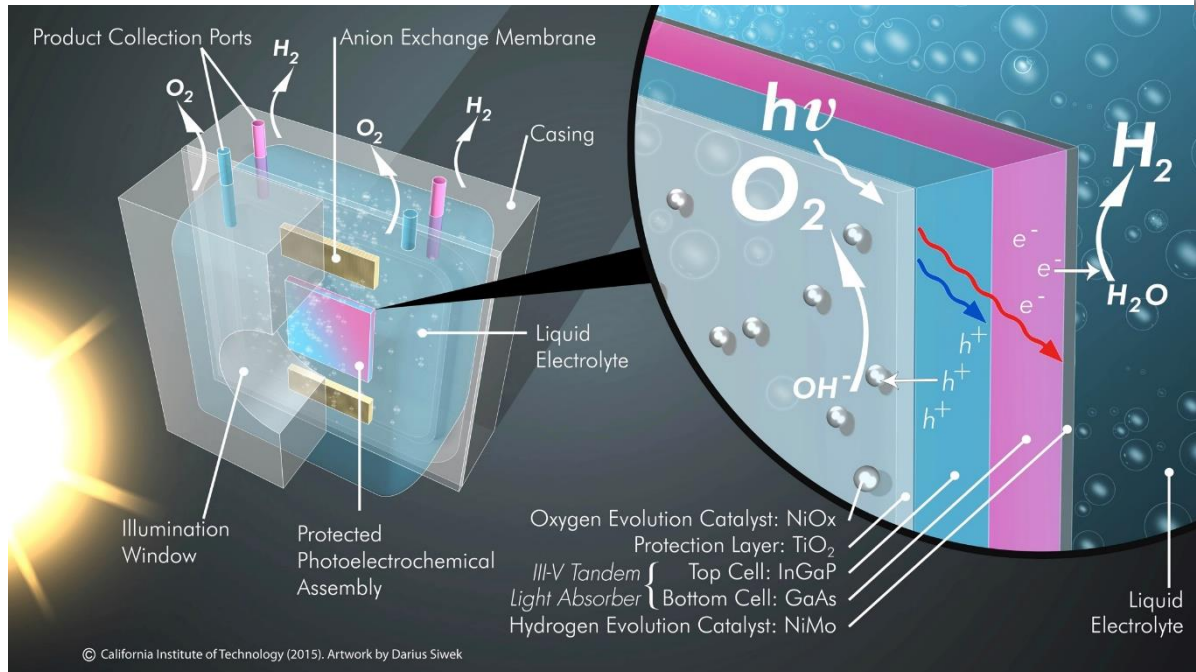


## JCAP'S FIRST PHASE: SOLAR FUELS FOR WATER-SPLITTING

### Oxide-Protected Photoanode Device:

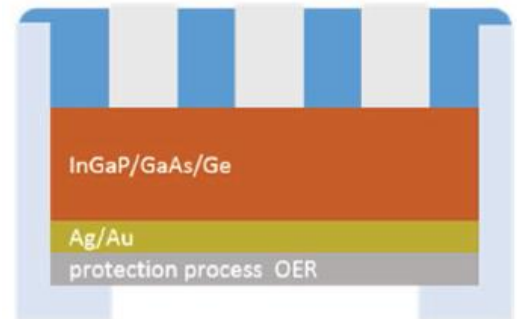
A >10% efficient, stable, unassisted solar-driven water-splitting in a monolithic photoelectrochemical system integrating

- protected tandem junction photoabsorbers,
- earth-abundant electrocatalysts, and
- anion exchange membranes.



*CX Xiang and Erik Verlage assemble a monolithically integrated III-V device, protected by a TiO<sub>2</sub> stabilization layer, which performs unassisted solar water splitting with hydrogen fuel and oxygen*

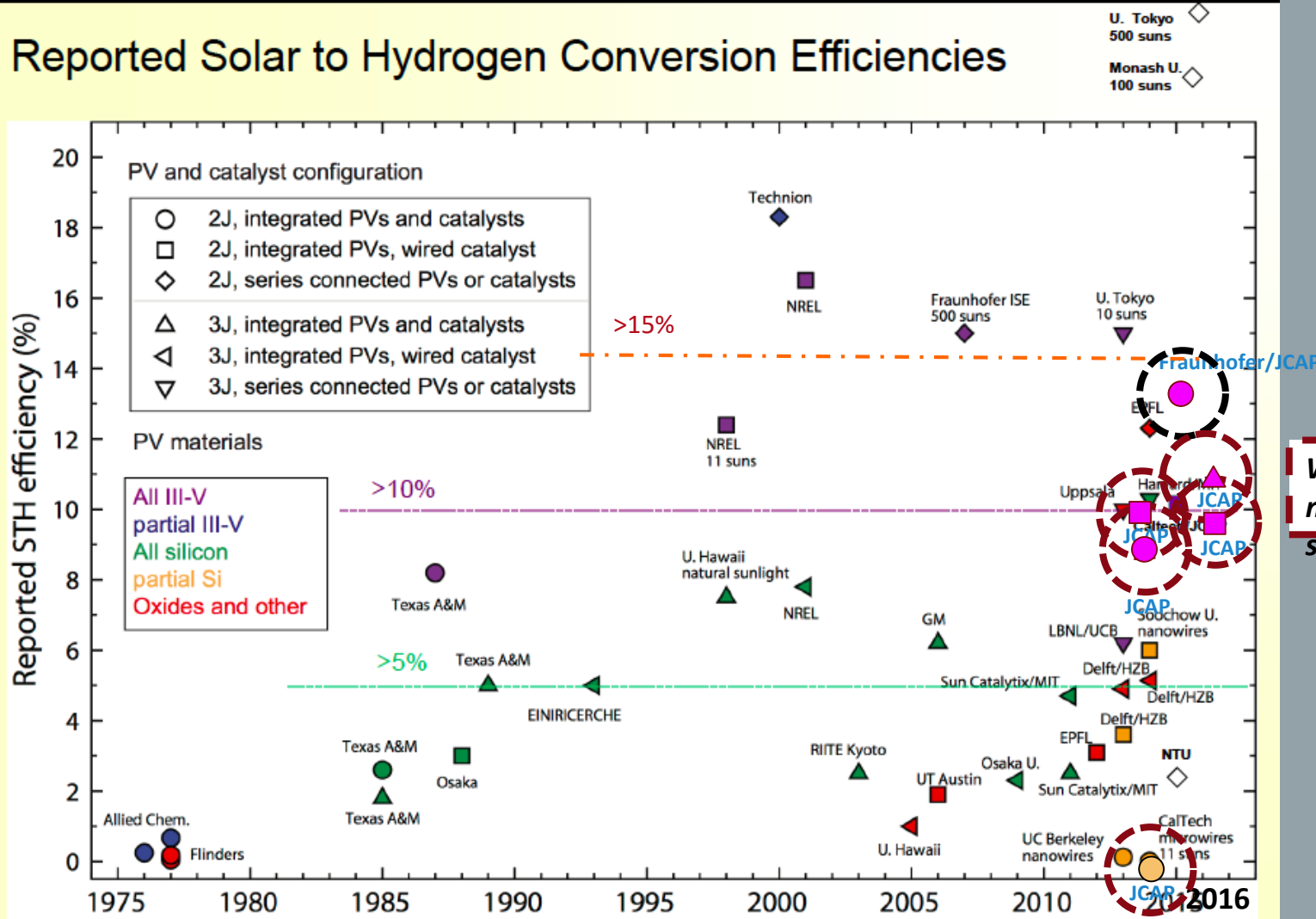
### Catalytic Grid Photocathode Device:



E. Verlage, S. Hu, R. Liu, R. J. R. Jones, K. Sun, C. Xiang, N. S. Lewis, Harry A. Atwater, *Energy Environ. Sci.*, 2015.  
K.A. Walczak, G.Segev, D.M. Larson, J.W. Beeman, F.A. Houle, and I.D. Sharp, *Adv. Energy Mater.*, 2017.

## STATE OF THE ART FOR PEC HYDROGEN GENERATION – 2015

## Reported Solar to Hydrogen Conversion Efficiencies

Ager, Shaner, Walczak, Sharp, Ardo, *Energy and Environmental Science*, 2015, 8, 2811

Ager, JCAP T3, 10/7/15 - 2

## PEC HYDROGEN GENERATION PERFORMANCE LIMITS

$$V_{PEC}(j) = \sum_i \ddot{A} V_{PV_i}(j) - V_{cat,a}(j) - V_{cat,c}(j) - V_{series}(j)^3 E_{rxn}$$

**PV Voltage:**  $V_{PV}(j) = \frac{n_d k_B T}{q} \ln \left( \frac{j}{j_0} \right) + 1$

**Catalyst Voltage:**  $V_{cat}(j) = \frac{RT}{\partial n_e F} \sinh^{-1} \left( \frac{j}{2j_{0,cat}} \right)$

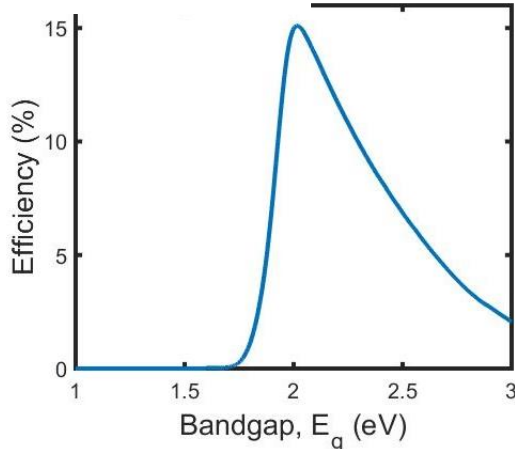
**Device operating point:**  $V_{op}(j_{op}) = E_{rxn}$

**Water splitting PEC efficiency:**  $\eta_{PEC} = \frac{j_{op} E_{rxn} f_{FE}}{P_{in}}$

## REALISTIC PERFORMANCE LIMITS FOR PEC HYDROGEN GENERATION

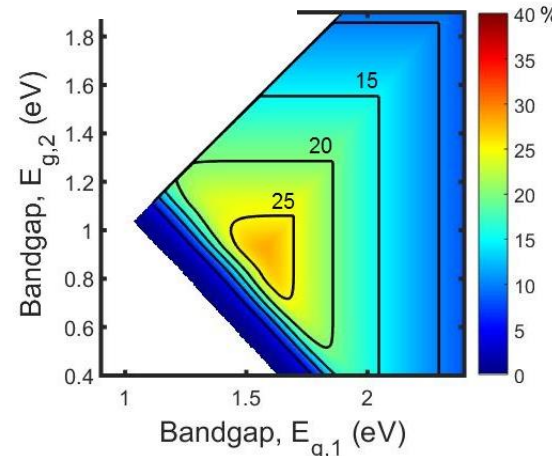
- Absorption of 90% of incident photons above the bandgap of the semiconductor
- An external radiative efficiency (ERE) of 3% (typical III-V)
- Catalytic exchange current densities of  $1 \text{ mA}\cdot\text{cm}^{-2}$  (HER) and  $10^{-3} \text{ mA}\cdot\text{cm}^{-2}$  (OER); consistent with the best reported values for Pt and  $\text{IrO}_2$
- Diode ideality factor,  $n_d$ , of 1.
- The electrochemical potential for water-splitting at standard conditions,  $E_{rxn}=1.23 \text{ V}$ .
- Unity Faradaic efficiency.

**Single Junction:**



$$\eta=15.1\%, E_g=2.05\text{eV}$$

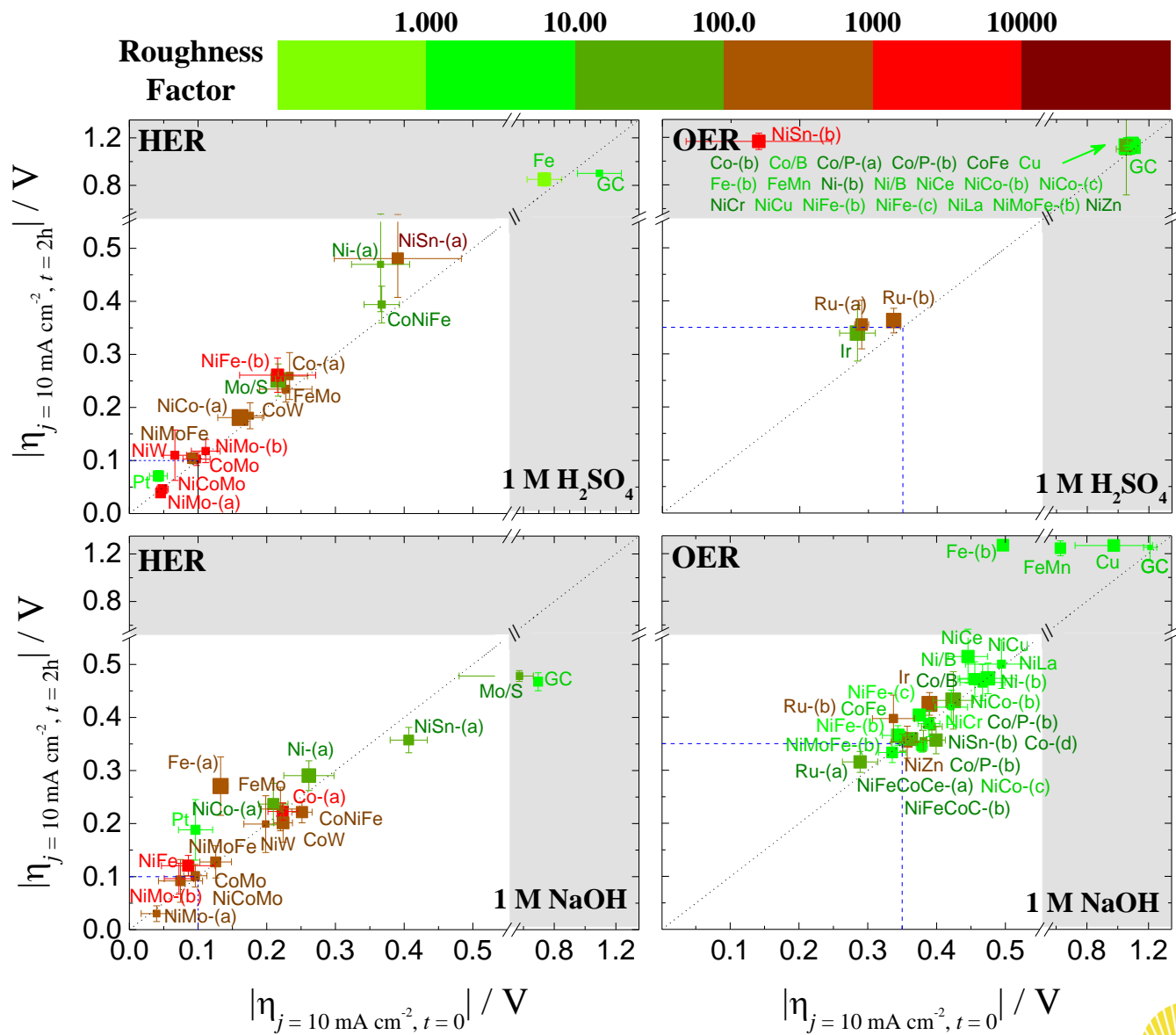
**Dual Junction:**



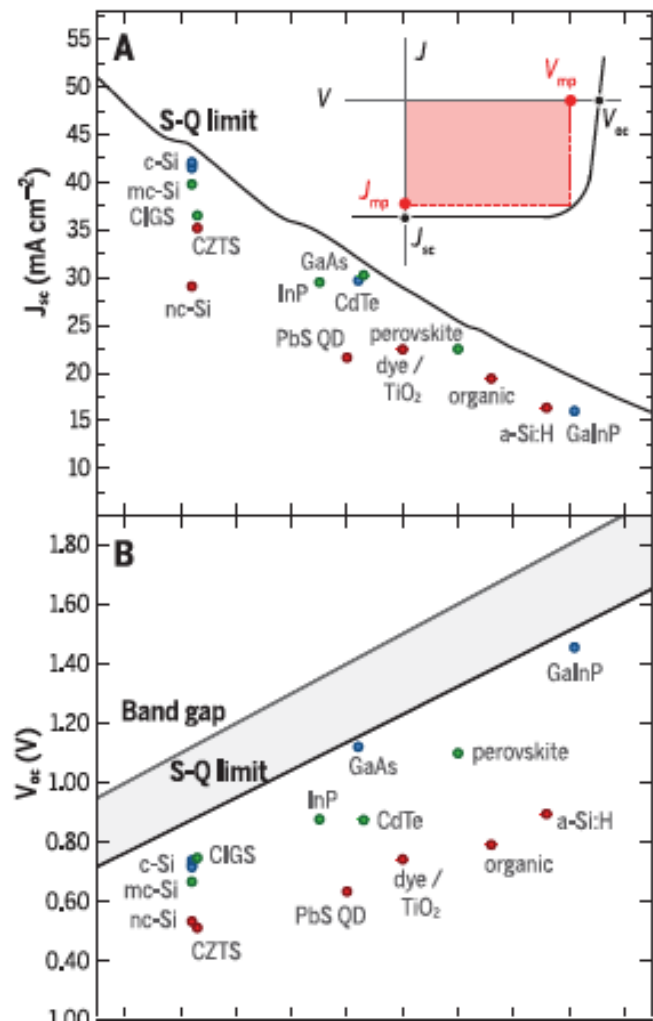
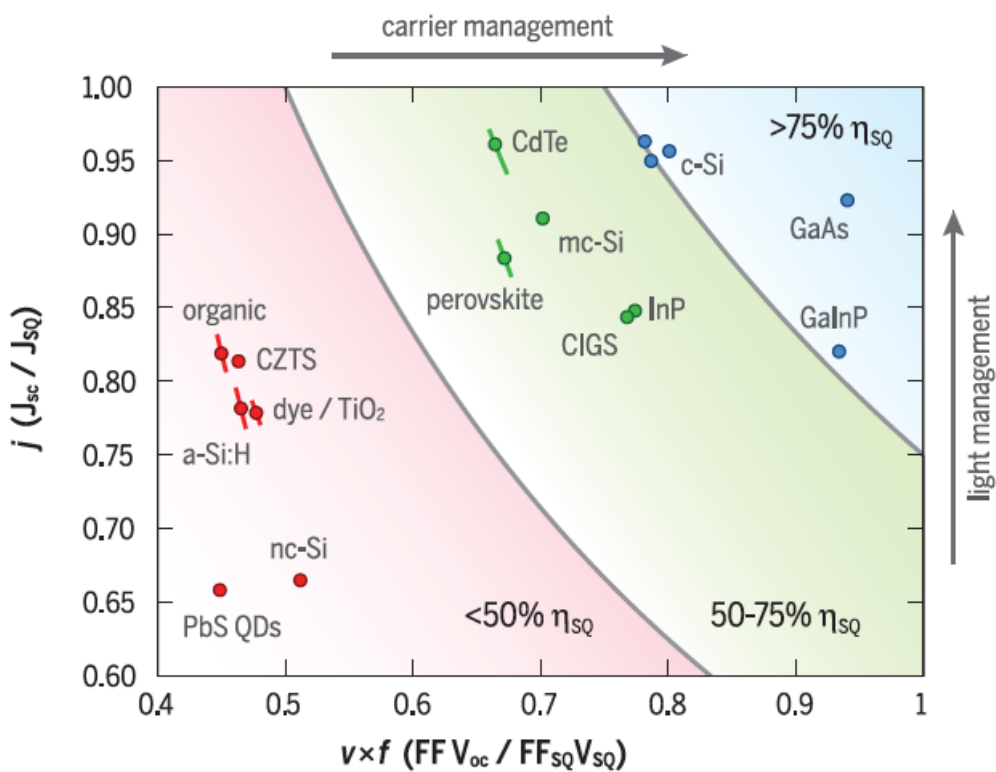
$$\eta=28.3\%, E_g=1.59, 0.92\text{eV}$$

Fountaine, Lewerenz, Atwater Nature Communications (2016)

## MATERIALS SELECTION: CATALYST BENCHMARKING

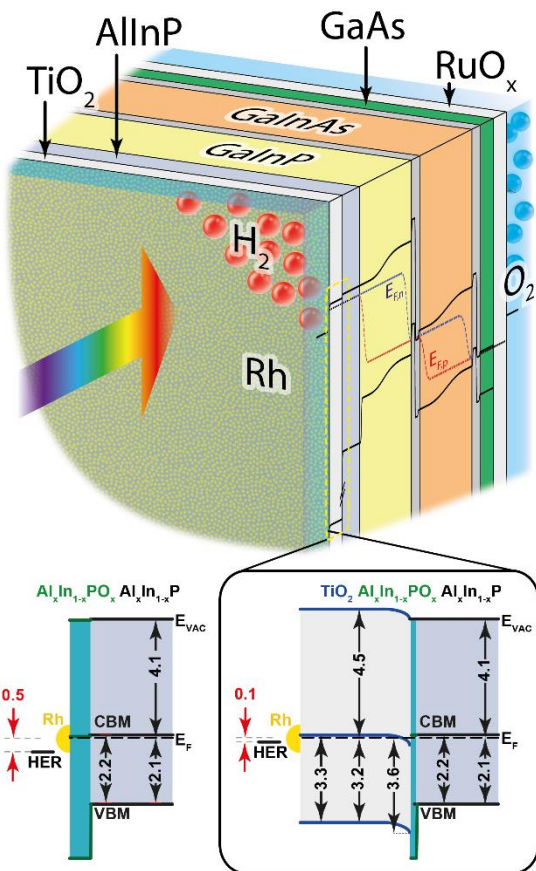


## MATERIALS SELECTION: PHOTOELECTRODES

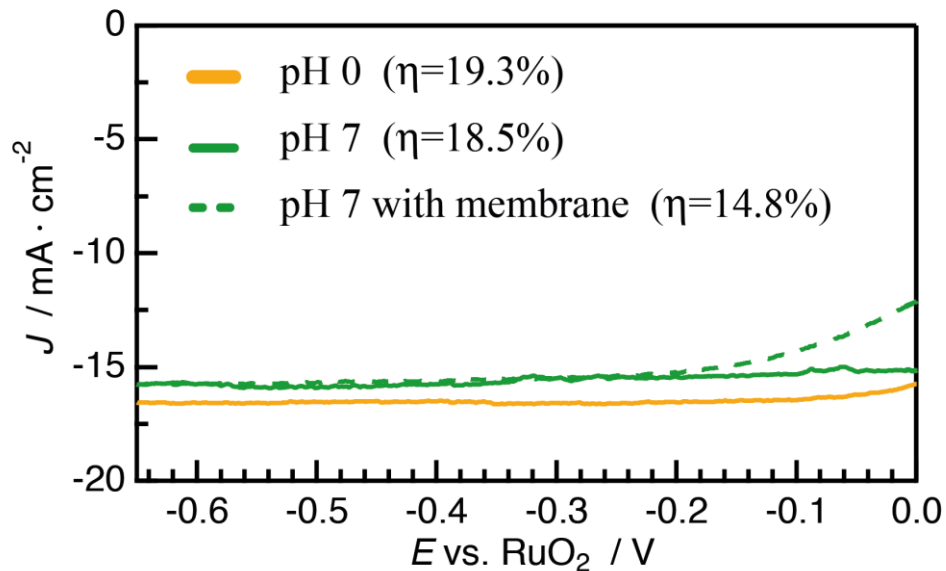


A. Polman, M. Knight, E.C. Garnett, B. Erhler and W.C. Sinke, Science (2016)

# 19.3% STH EFFICIENCY INTEGRATED PEC DEVICE

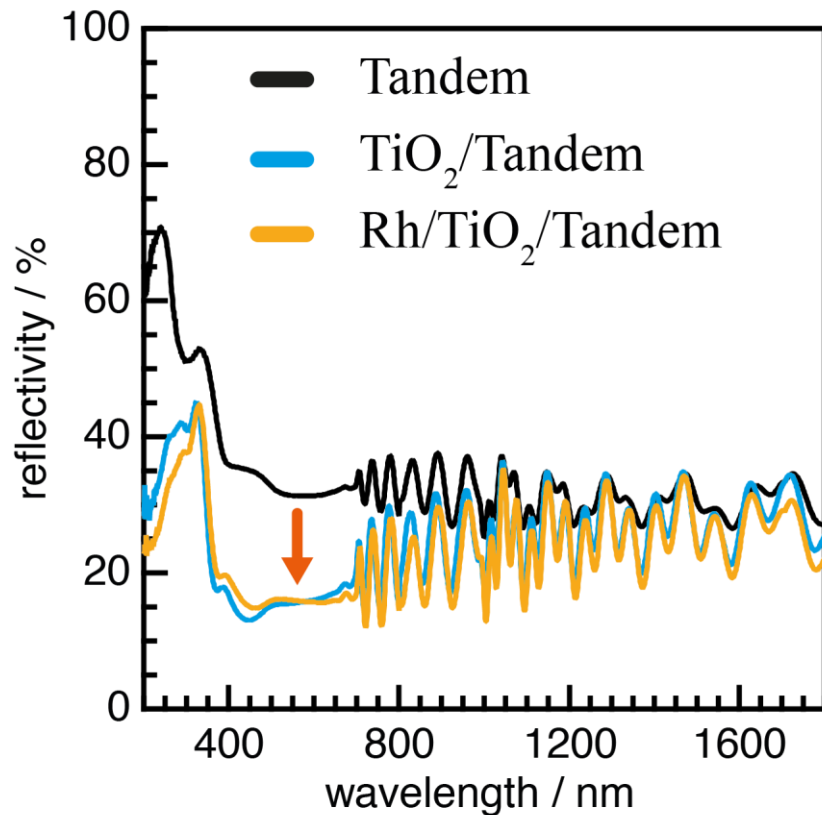
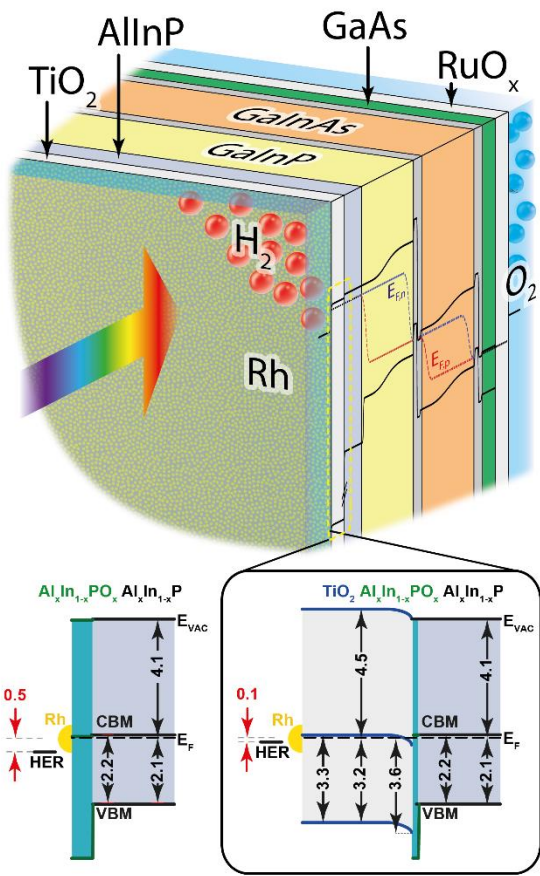


$\text{GaInP}$  with  $E_g = 1.78 \text{ eV}$ ;  $\text{GaInAs}$  with  $E_g = 1.26 \text{ eV}$



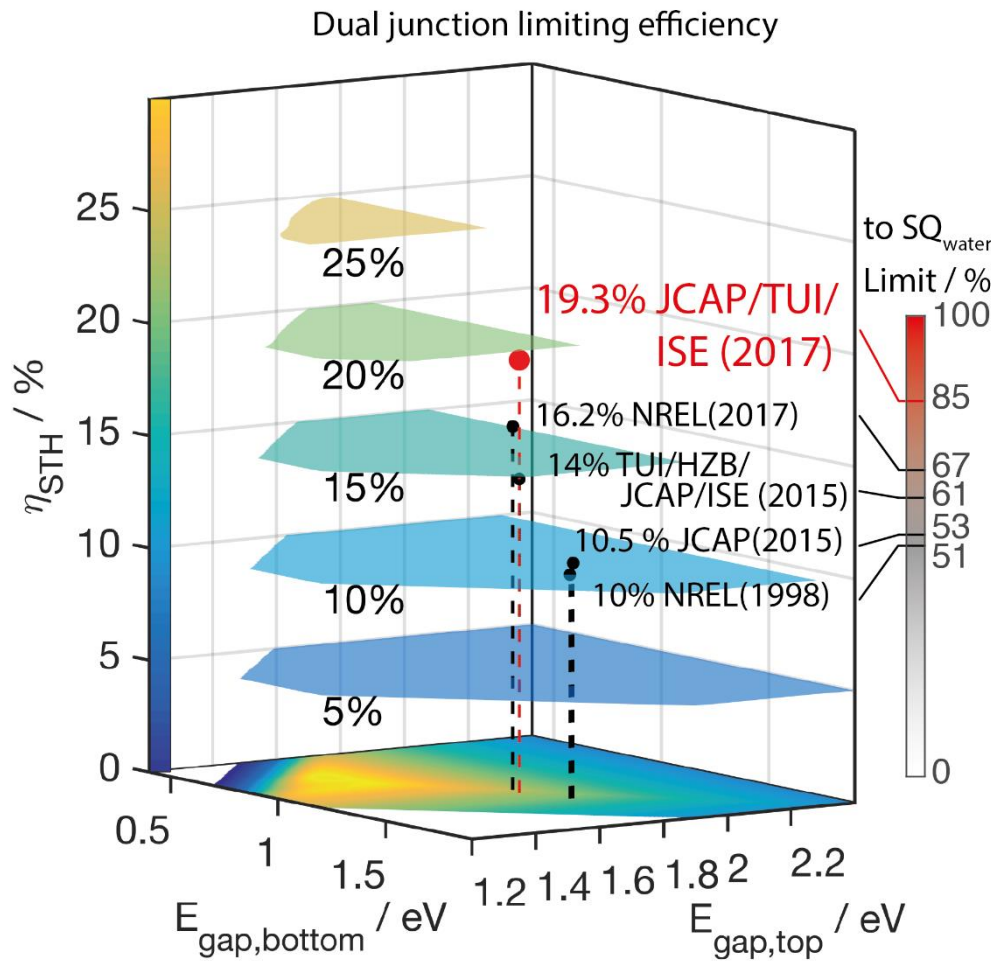
W.H. Cheng, M.H Richter, M.M May, J. Ohlmann, D. Lackner, F. Dimroth, T. Hannappel, H.A. Atwater, and H.J. Lewerenz, ArXiv 2017

## 19.3% STH EFFICIENCY INTEGRATED PEC DEVICE



W.H. Cheng, M.H Richter, M.M May, J. Ohlmann, D. Lackner, F. Dimroth, T. Hannappel, H.A. Atwater, and H.J. Lewerenz, ArXiv 2017

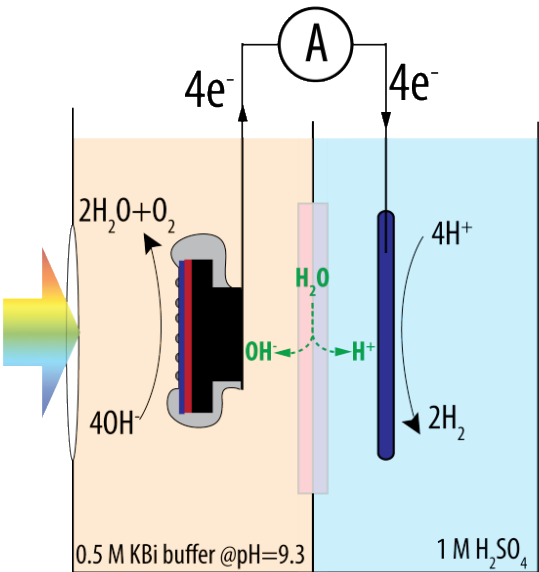
## RAPID ADVANCES IN EFFICIENCY OF INTEGRATED STH PECs



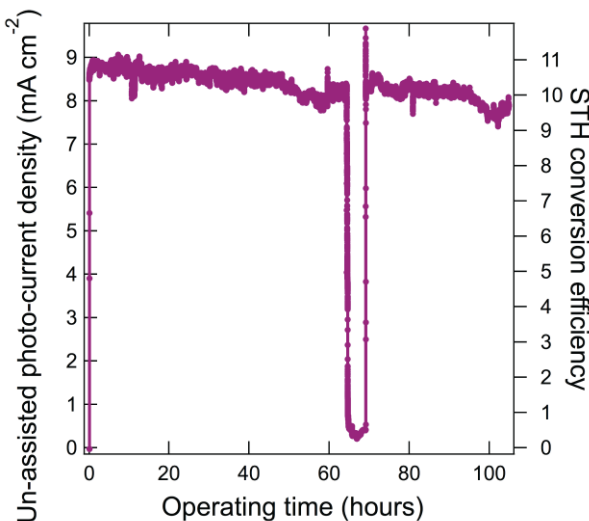
W.H. Cheng, M.H Richter, M.M May, J. Ohlmann, D. Lackner, F. Dimroth, T. Hannappel, H.A. Atwater, and H.J. Lewerenz, ArXiv 2017

# UNASSISTED WATER SPLITTING WITH BIPOLAR MEMBRANE AT 10% ENERGY CONVERSION EFFICIENCY

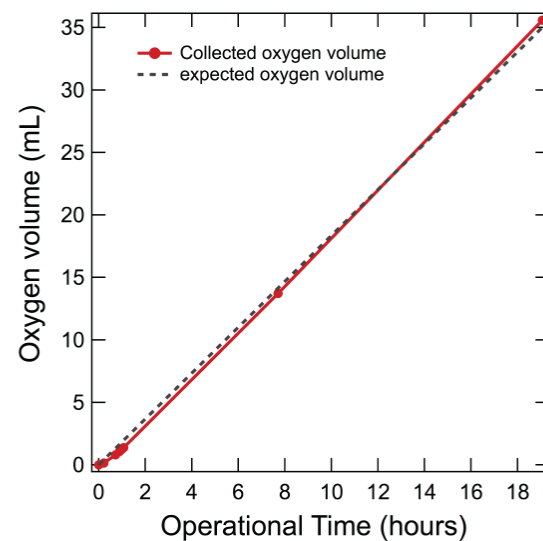
Schematic illustration of a bipolar membrane device



Un-assisted solar-driven water-splitting performance



Product gas collection performance



All earth-abundant electrocatalysts:  $\text{NiO}_x$  for DER in the KBi buffer and  $\text{CoP}_x$  for HER in  $1.0 \text{ M H}_2\text{SO}_4$ .

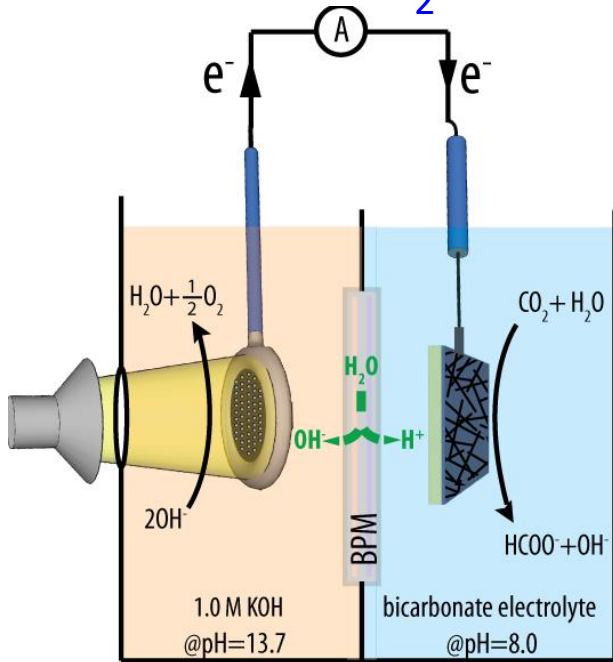
- $> 1.0 \text{ cm}^2$ ,  $> 10\%$  STH conversion efficiency,  $> 100$  hour stability was achieved using a tandem photoabsorber in a cell configuration that incorporates a bipolar membrane.
- The acid stable electrocatalyst, CoP, was successfully integrated into the cell.

Bipolar membrane:

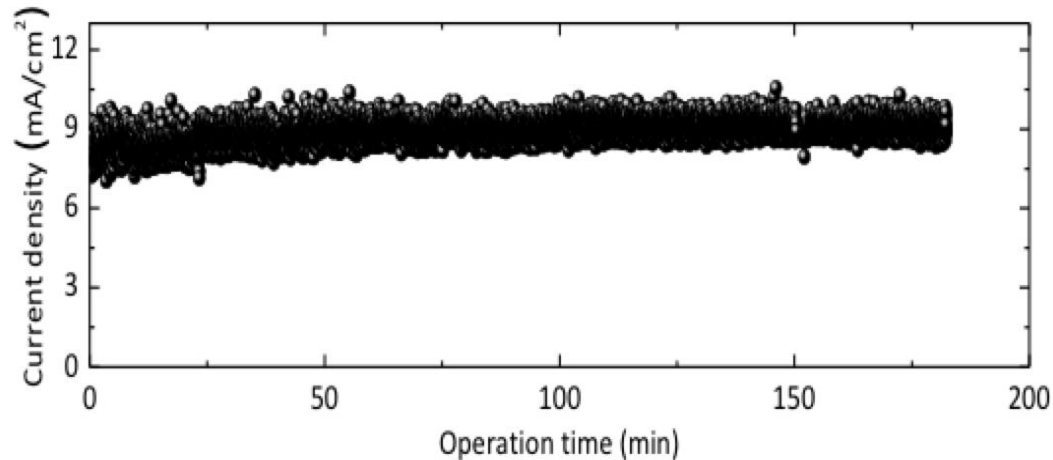
- near-unity transference numbers for proton and hydroxide transport at relatively high operational current densities
- $\sim 400\text{-}500 \text{ mV}$  voltage loss due to ohmic resistance, water dissociation and water transport processes, further improvements can be made by incorporating water dissociation catalysts at the interface.

## SOLAR-DRIVEN REDUCTION OF CO<sub>2</sub> TO FORMATE AT 10% ENERGY CONVERSION EFFICIENCY

Schematic illustration of the series connected photoanode and dark cathode for CO<sub>2</sub> reduction to formate



Un-assisted solar to formate conversion efficiency at 10% under 1.0 Sun illumination



Best combination of catholyte and anolyte to achieve the lowest total overpotential for the device

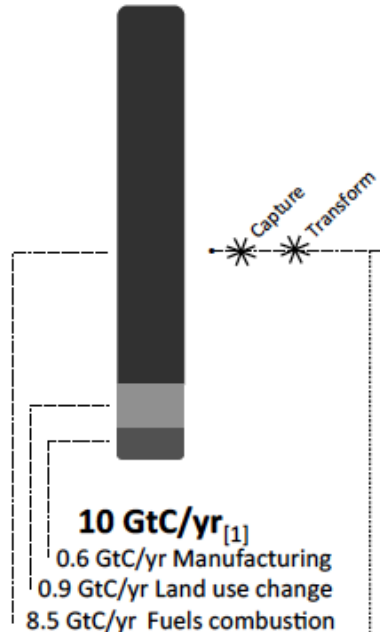
Minimal product crossovers even at high formate concentration

- Photoanode: InGaP/GaAs/TiO<sub>2</sub>/NiO<sub>x</sub> at pH=14 electrolyte previously used for solar water-splitting.
- Dark cathode: Pd/C nanoparticles on Ti mesh in pH=8 bicarbonate solution achieved  $\leq 100$  mV overpotential and >94% Faradaic efficiency at 10 mA cm<sup>-2</sup>.
- Bipolar membrane sustained the steady-state pH differential and minimized the product crossovers.

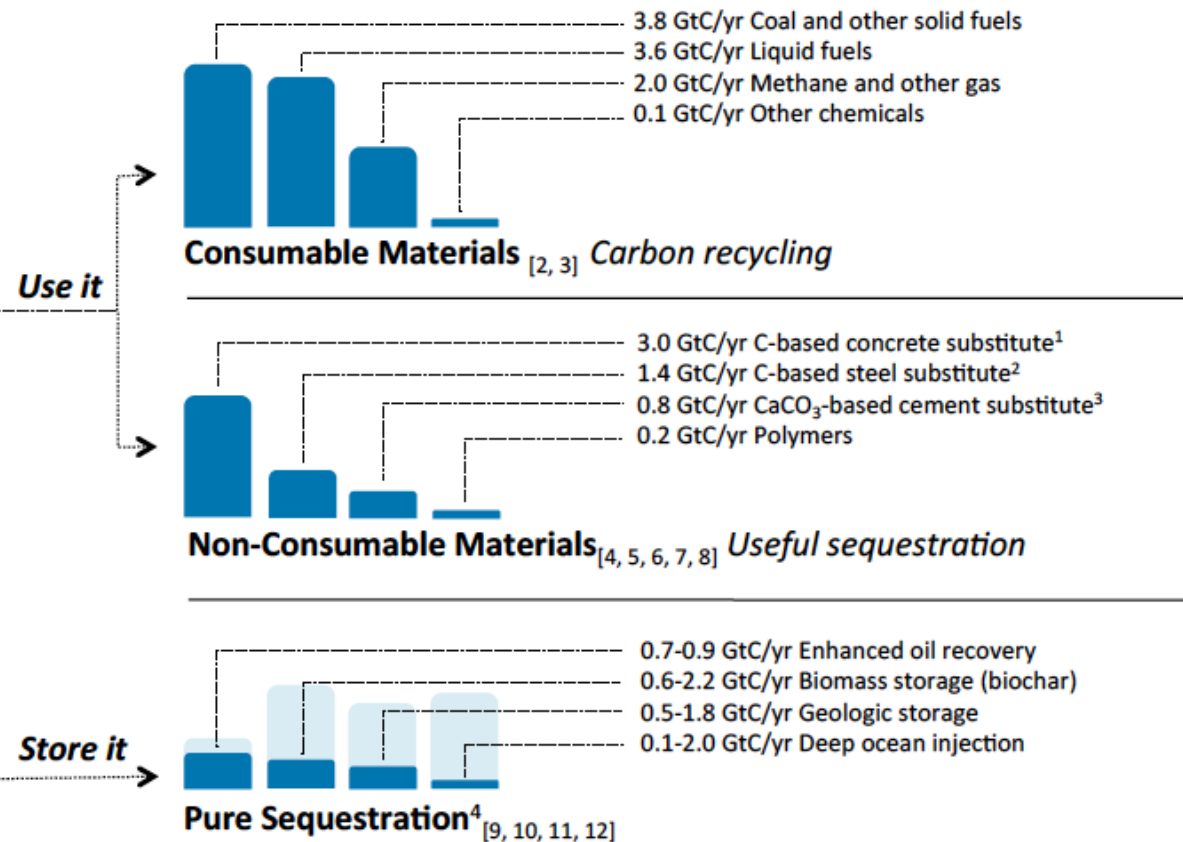
CX Xiang, et.al. ACS Energy Lett., 2016, 1, pp 764–770

## RELATIVE SCALE OF EMISSIONS AND POTENTIAL USES FOR CO<sub>2</sub>

### Current emissions:



### Some possible non-atmospheric ends:



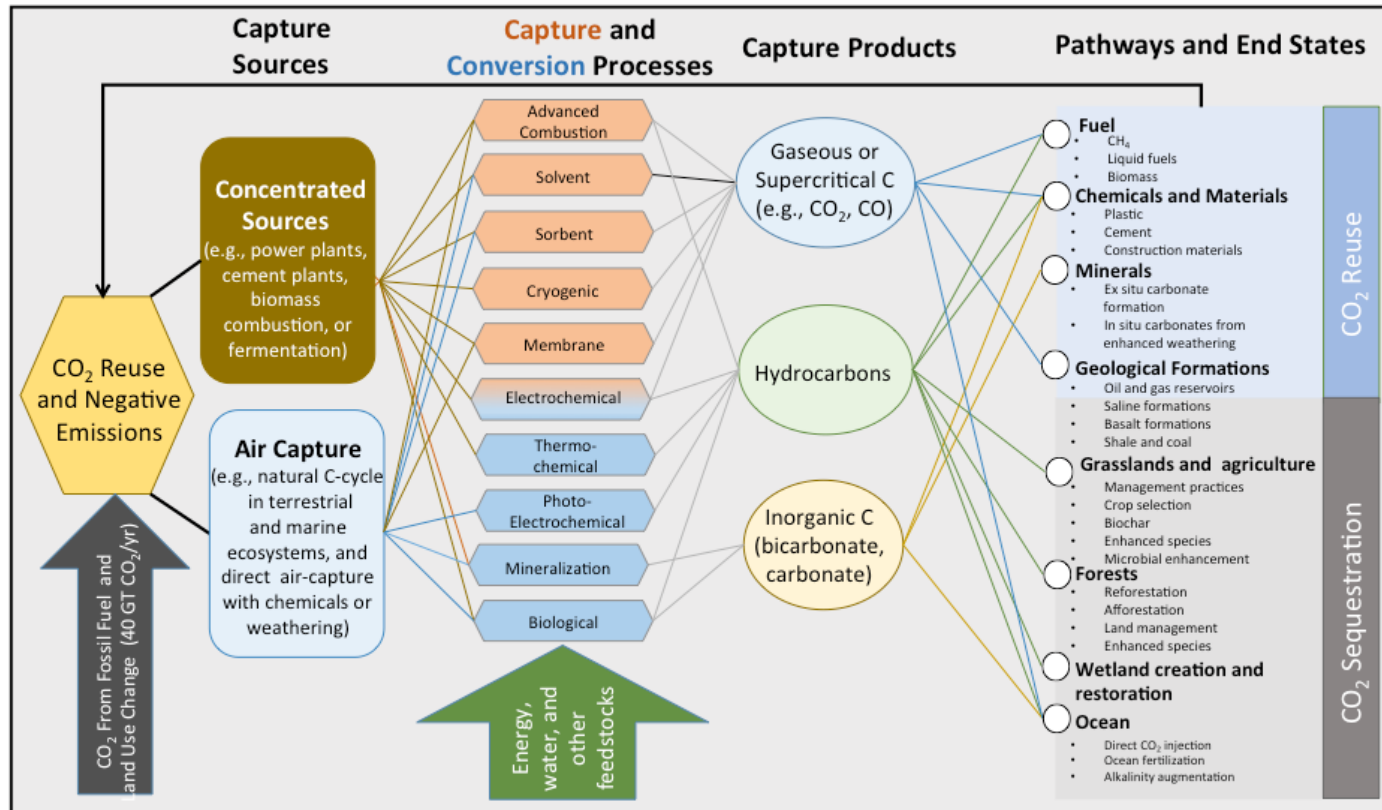
GtC = 1 billion metric tons of carbon equivalent, i.e. 1Gt MeOH =  $12.01/(12.01+16.00+4*1.01)$  Gt = 0.37 GtC.

<sup>1</sup> Assuming cement is composed of CaCO<sub>3</sub>, and the aggregate is composed of 50% CaCO<sub>3</sub> by mass • <sup>2</sup> Assuming a steel substitute that is similar in composition to carbon fiber, i.e. 90% C by mass.

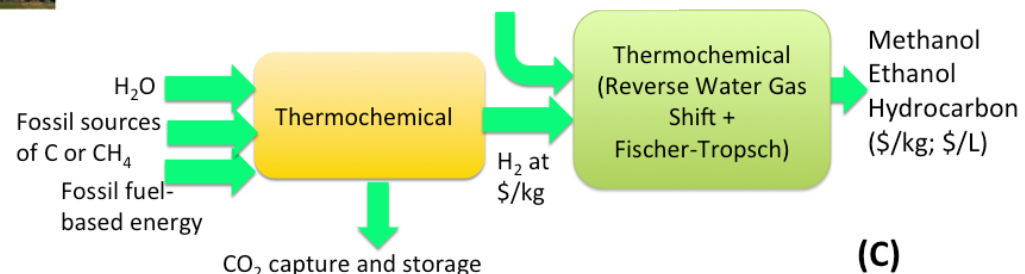
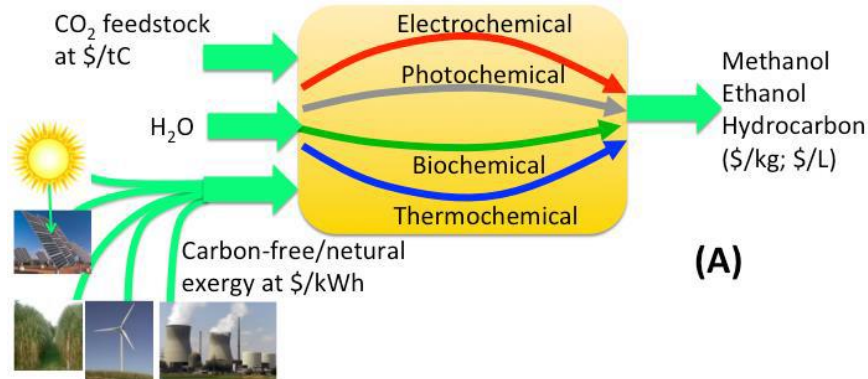
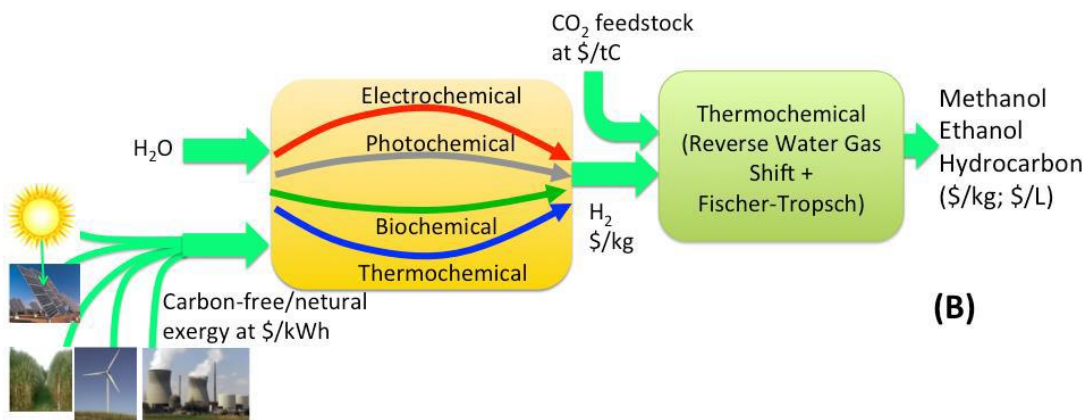
<sup>3</sup> Assuming cement is composed of CaCO<sub>3</sub> • <sup>4</sup> Estimated feasible scale-up rates by 2050, excluding geoengineering approaches. Shaded bars indicate the upper range of estimates.

## THE CO<sub>2</sub> UTILIZATION LANDSCAPE

- Focus on processes able to capture, reduce or sequester 1 GtCO<sub>2</sub>/yr scale
- 1 of the top 5 Priorities: Synthetic Transformations of CO<sub>2</sub>
- Recommendations:
  - Reduce the cost of carbon-free/neutral energy in the form of heat/electricity
  - Focus on fundamentals of electrocatalysis and photoelectrocatalysis
  - Identify catalysts made of abundant elements that reduce the overpotentials for CO<sub>2</sub>RR and OER at high reaction rates.

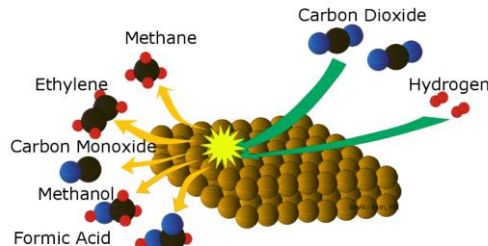


Secretary of Energy Advisory Board Report, 12/13/2016

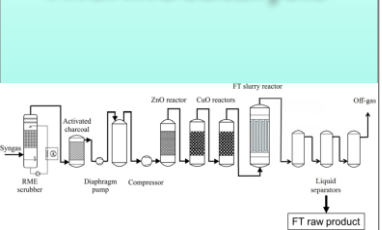
THE CO<sub>2</sub> UTILIZATION LANDSCAPE

# ROUTES TO FUELS FROM CO<sub>2</sub>: COMPARING APPROACHES

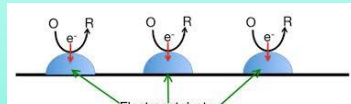
Approaches to reduction of CO<sub>2</sub> to fuels:



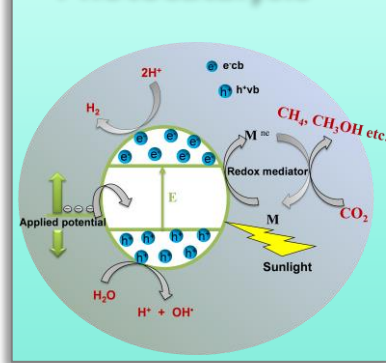
## Thermocatalysis



## Electrocatalysis



## Photocatalysis



## Biocatalysis



### Advantages:

Mature technology; heat only required as energy input

### Disadvantages:

High capital cost and intrinsically large-scale for plant; efficiency < 100%

Room temperature operation, high FE and throughput for certain products (e.g., CO, HCOO<sup>-</sup>)

Limited throughput, low selectivity and STF efficiency for alkane and alcohol fuels

Low capital cost, scalable, uses sunlight as direct energy input

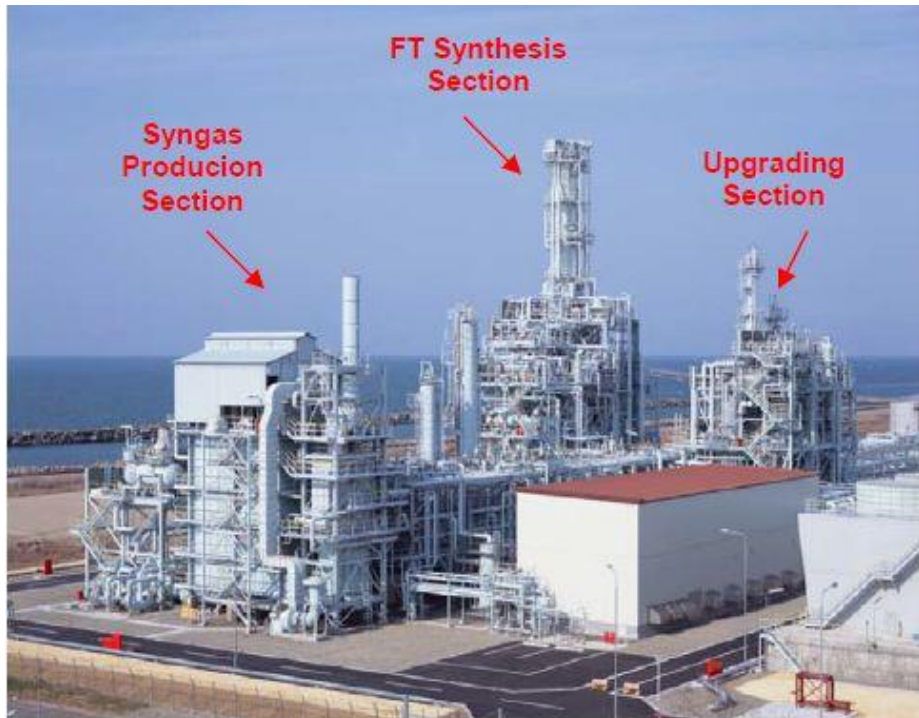
Low efficiency and selectivity, product separation

Low capital cost; near room temperature; near neutral pH operation

Limited durability (bacteria die after 30 days); limited pH range, low throughput

## WHY NOT JUST MAKE CO AND H<sub>2</sub> AND USE THERMOCHEMISTRY TO DO THE REST?

- High capital cost for thermochemical plant
- Fischer-Tropsch thermal conversion efficiency 50-60%
- Requires source of hydrogen using process other than steam reforming (PEC water splitting technology development ongoing)



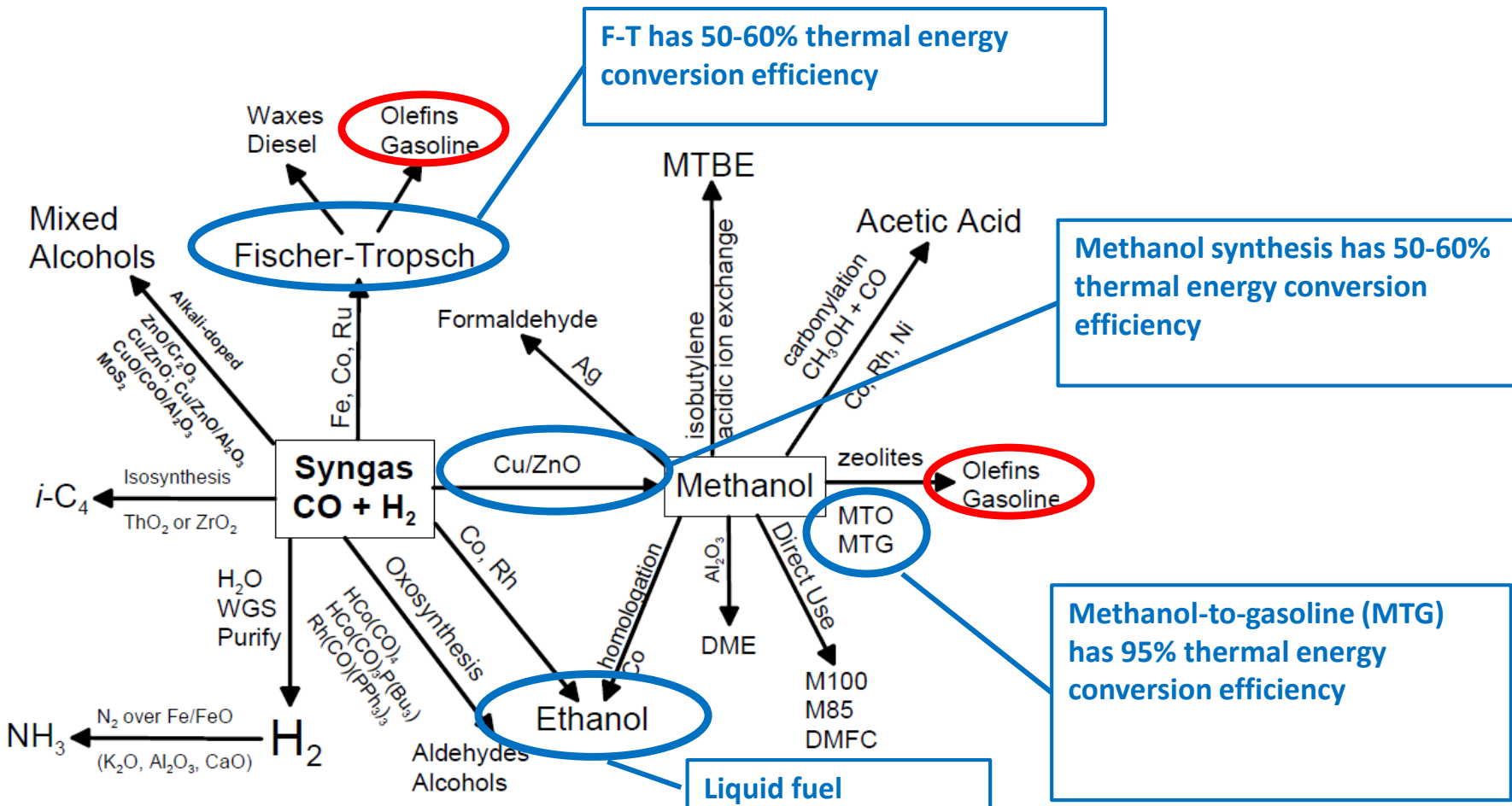
Japanese Gas to Liquids Pilot Plant, Niigata City, Japan

Production scale: 500 barrels/day

*JCAP aims for direct, selective CO<sub>2</sub>R catalysis strategies under mild P & T conditions that have potential for scalable production of fuels from sunlight with low capital cost.*

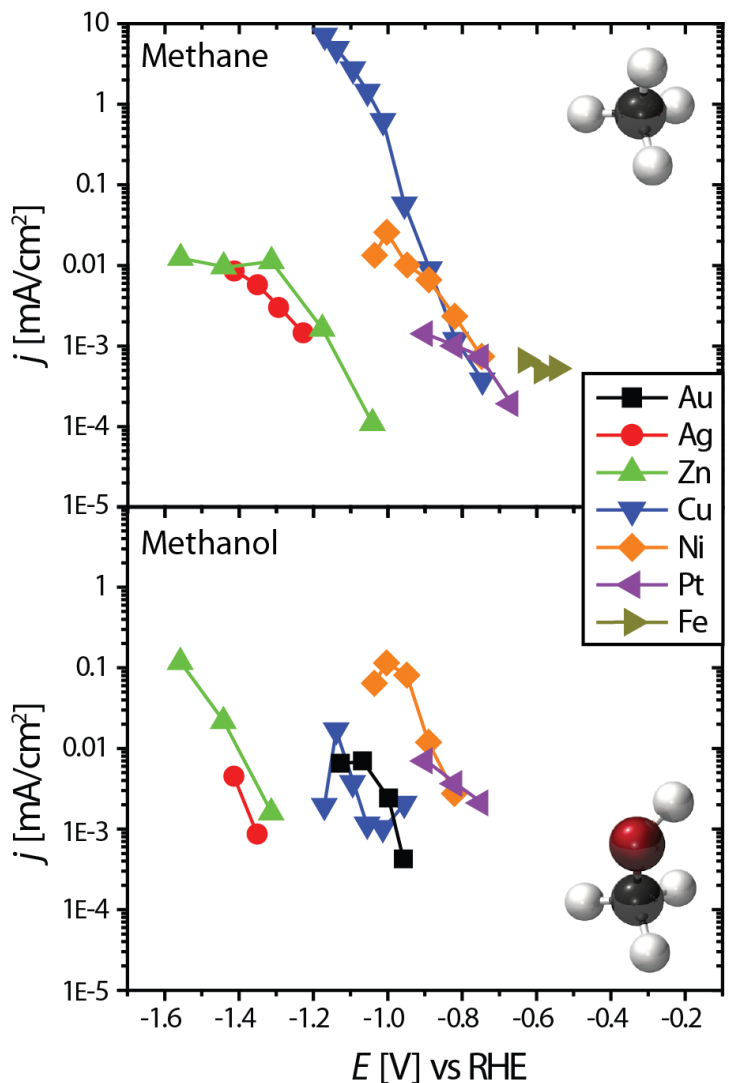
## CHEMICAL SYNTHESES FROM SYNGAS AND METHANOL

- Many chemical conversions from syngas to products, including gasoline via Fischer-Tropsch
- Many chemical conversions from methanol to products, including gasoline
- Methanol is an achievable product from CO<sub>2</sub>R PEC

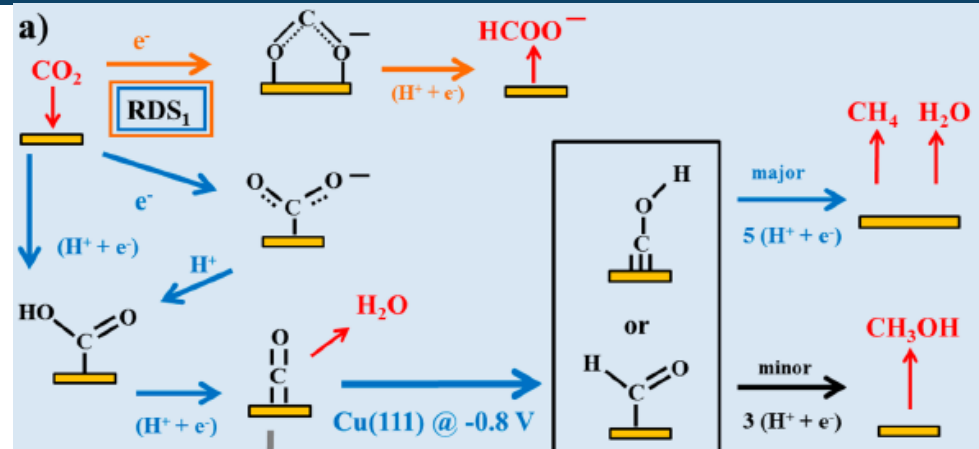
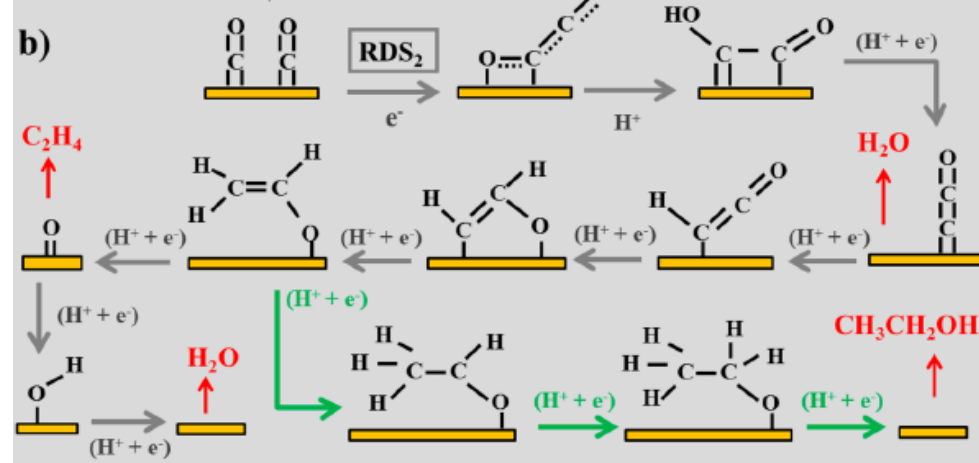
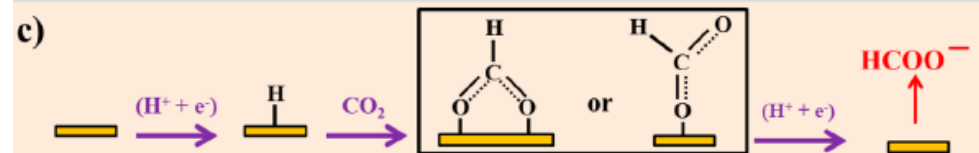


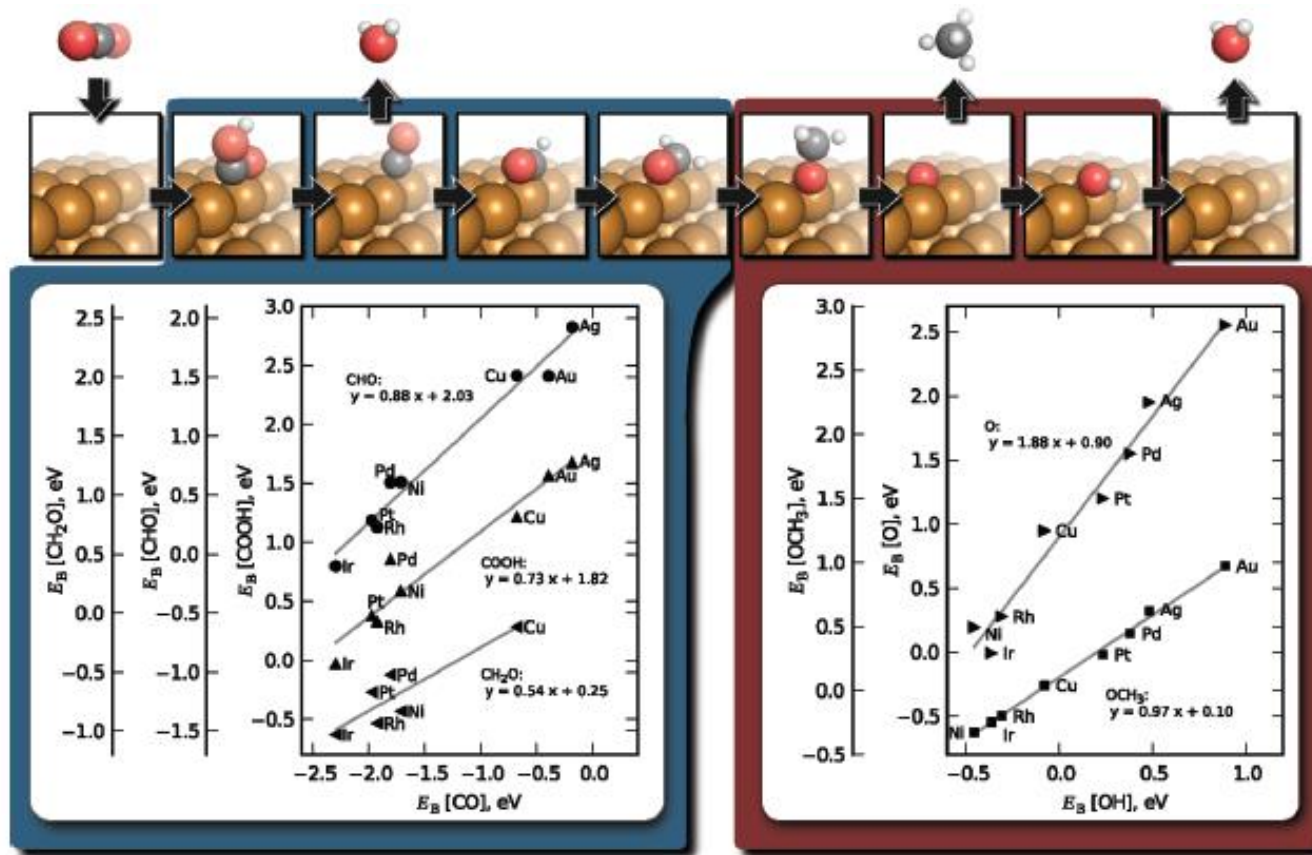
Source: P.L. Spath and D.C. Dayton, Preliminary screening—technical and economic assessment of synthesis gas to fuels and chemicals with emphasis on the potential for biomass-derived syngas, National Renewable Energy Laboratory, NREL/TP-510-34929, December, 2003.

## CU IS THE BEST ELEMENTAL CATALYST – SO FAR



Selectivity is a major issue:  
Competition with HER

POSSIBLE PATHWAYS FOR CO<sub>2</sub> REDUCTION CATALYSIS ON COPPER*C<sub>1</sub> Products: CO<sub>2</sub> Adsorption**C<sub>2</sub> Products: CO Dimerization**C<sub>1</sub> Products: CO<sub>2</sub> Insertion*

SCALING RELATIONSHIPS FOR CO<sub>2</sub> INTERMEDIATES ON CU

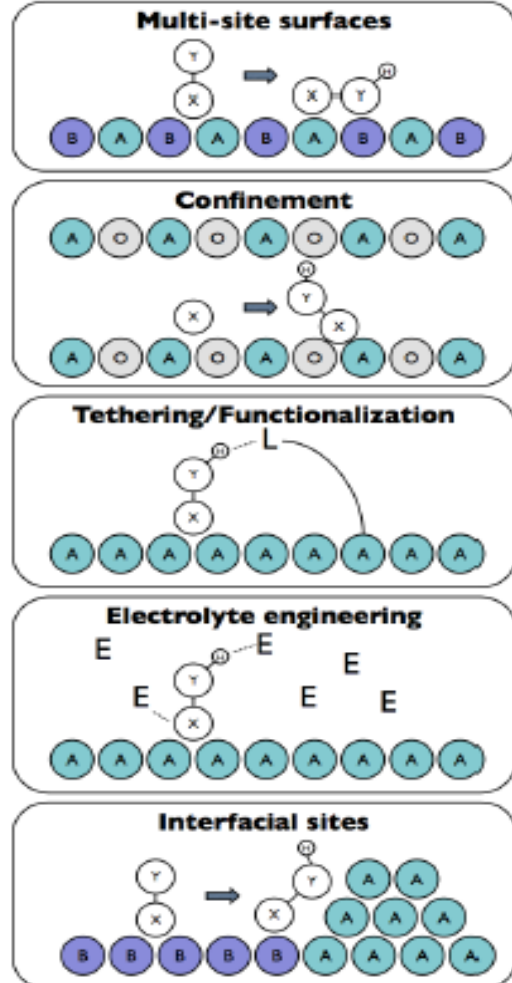
Adsorption energies of the key bound intermediates on fcc Cu (211)

Adsorption energies of adsorbates binding through oxygen

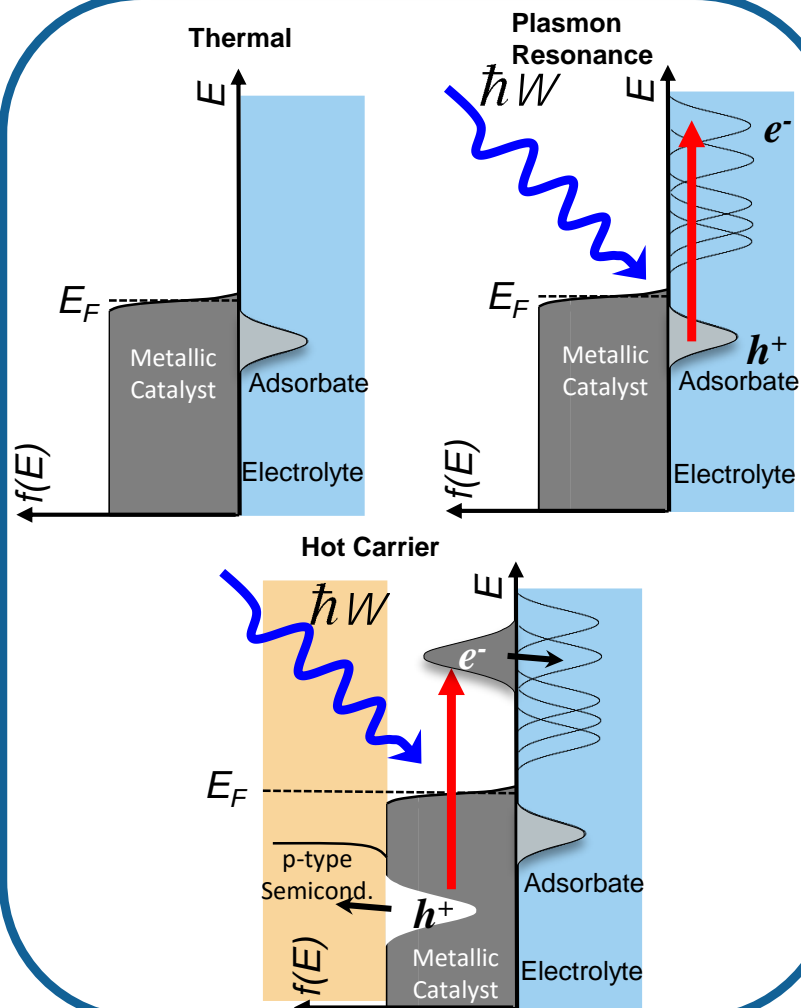
Peterson and Nørskov, J Phys Chem Lett., 3, 251–25 (2012).

OVERCOMING SCALING RELATIONSHIPS FOR CO<sub>2</sub> REDUCTION

## Electrocatalysis Strategies

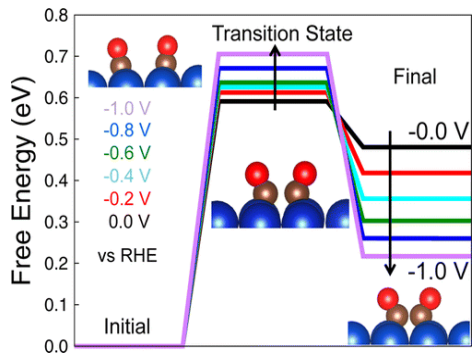


## Photocatalysis Strategies

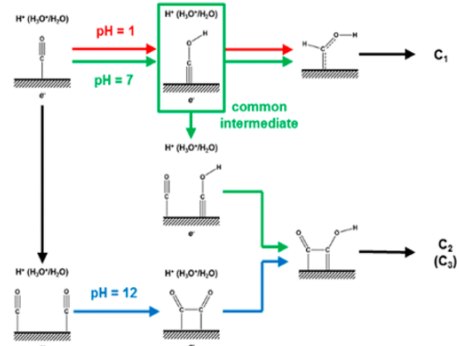


## THEORY DEVELOPMENTS

## Kinetics and Mechanisms



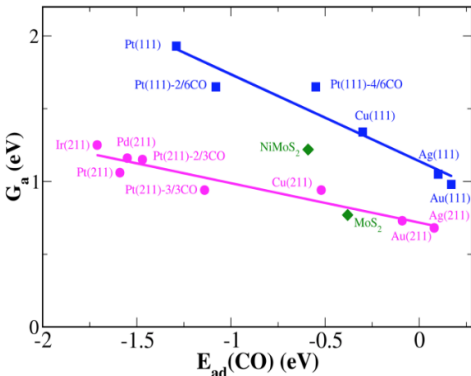
J.D. Goodpaster, A.T. Bell, and M. Head-Gordon, *J. Phys. Chem. Lett.*, **2016**, 7, 1471-1477.



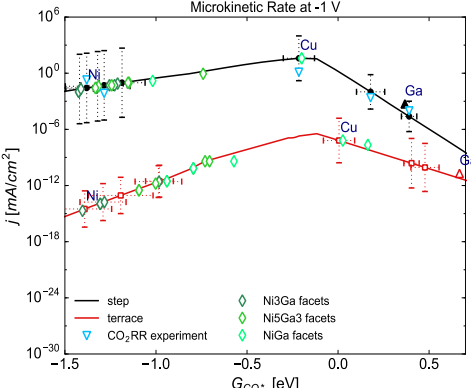
W.A. Goddard et al., *JACS*, **2016**, 138, 483-486.

W.A. Goddard et al. *J. Phys. Chem. Lett.*, **2015**, 6, 4767-4773.

## Catalyst Screening

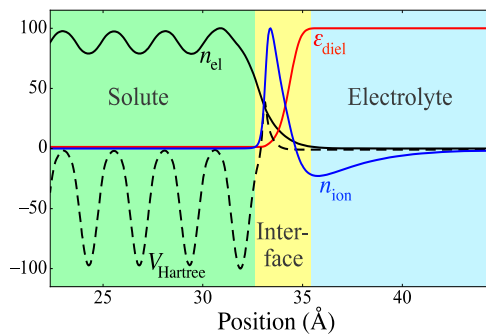


J. Xiao, X. Liu, K. Chan, and J.K. Nørskov, **2016**.  
J.K. Nørskov et al., *ACS Catalysis*, **2016**, 6, 4428-4437.

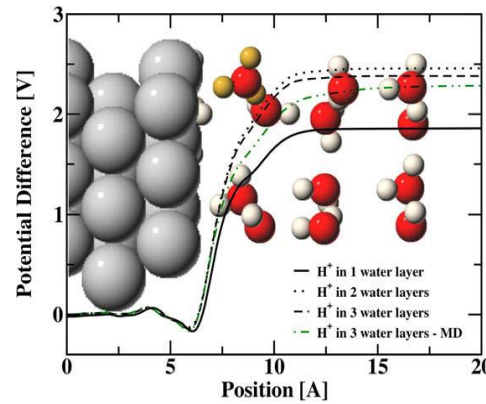


Z.W. Ulissi, M.T. Tang, K. Chan, and J.K. Nørskov, **2016**.

## Electrochemical Interface and Higher Order Methods



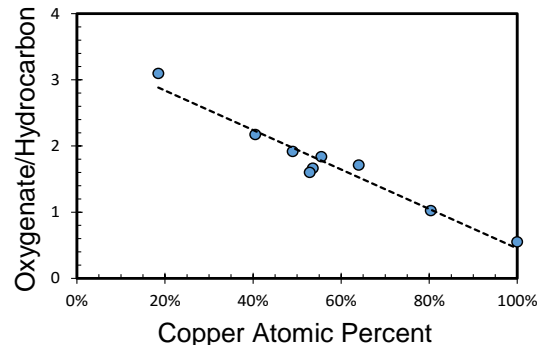
K. Mathew and R.G. Hennig, **2016**,  
<https://arxiv.org/abs/1601.03346>



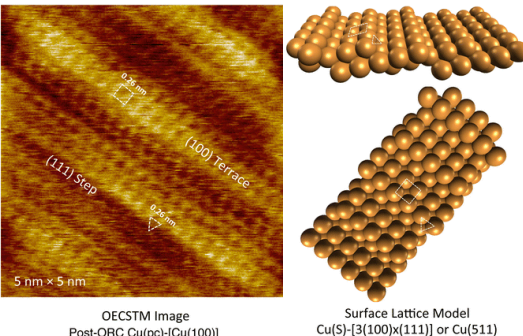
J.K. Nørskov et al., *Chem. Phys. Lett.*, **2008**, 466, 68-71.

## EXPERIMENTAL DEVELOPMENTS

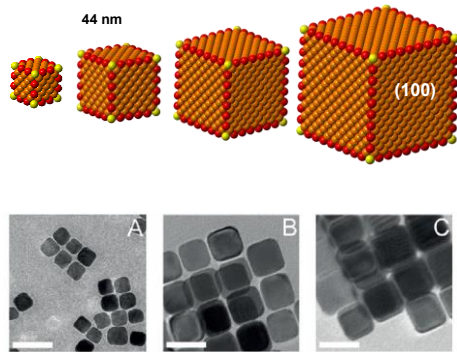
## Catalyst Composition

E.L. Clark and A.T. Bell *et al.*, 2016.

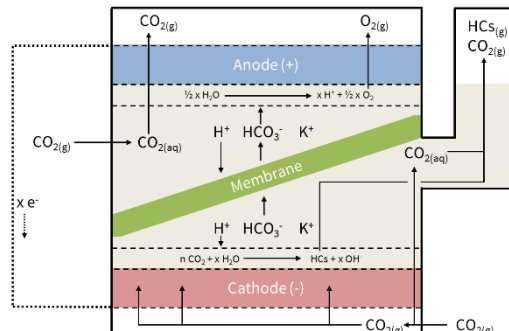
## Catalyst Surface Structure

Y.G. Kim, A. Javier, J.H. Baricuatro, and M.P. Soriaga, *Electrocatal.*, 2016, 7, 391-399.

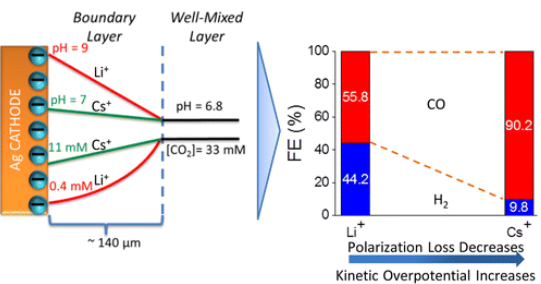
## Catalyst Morphology

A. Lojudice, P. Lobaccaro, J.W. Ager, and R. Buonsanti, *Angew. Chem.*, 2016, 55, 5789-5792.

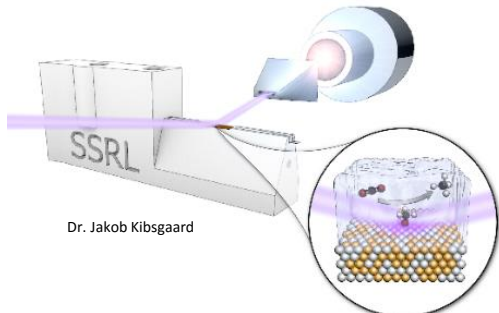
## Reactor Design

J.T. Feaster, C. Hahn, and T.F. Jaramillo *et al.*, 2016.

## Electrolyte Composition and Ionomer-Catalyst Interactions

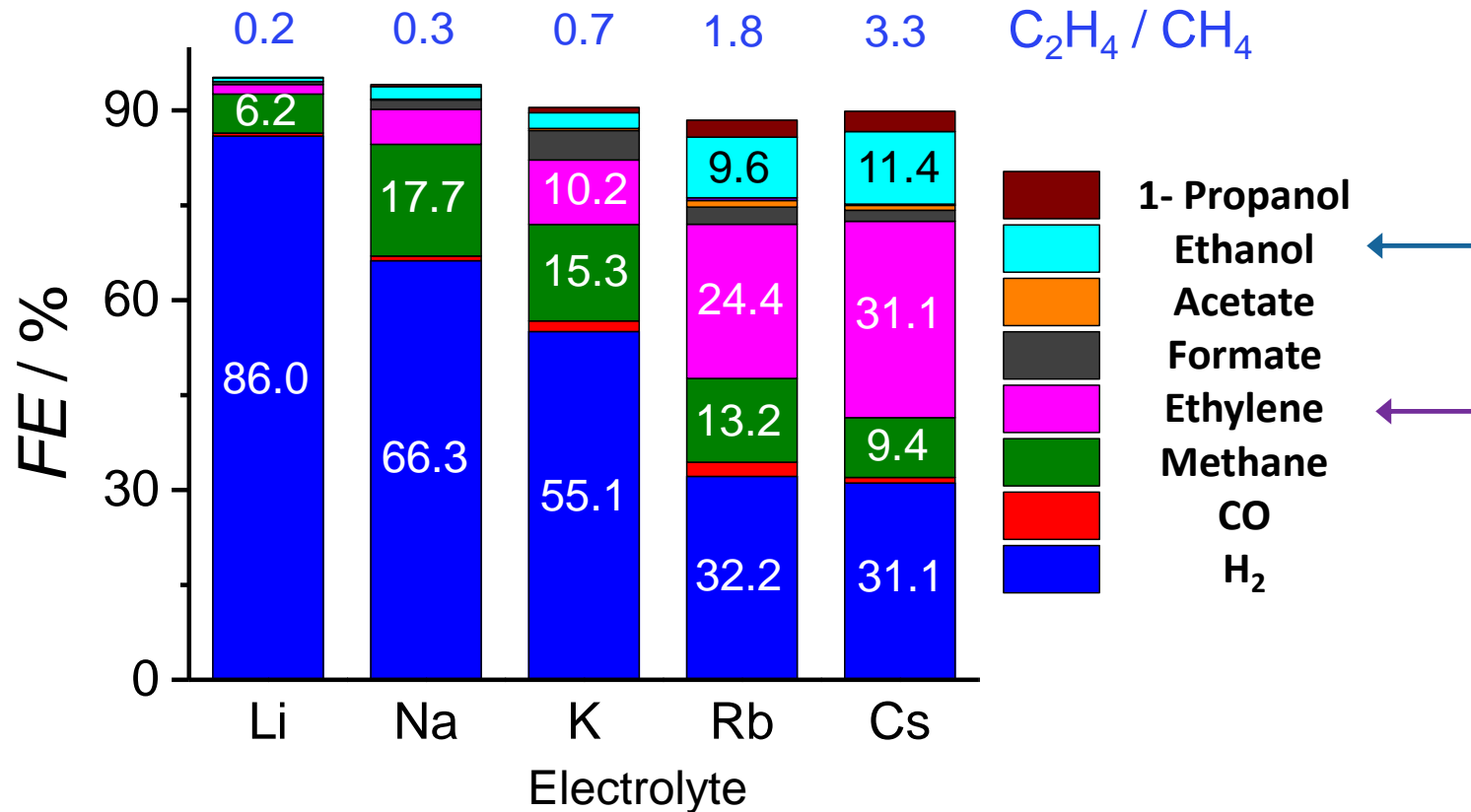
M.R. Singh, Y. Kwon, Y. Lum, J.W. Ager, and A.T. Bell, *J. Am. Chem. Soc.*, 2016, 138, 13006-13012.

## Catalyst and Reaction Intermediate Characterization

J.T. Feaster, J. Yano, T.F. Jaramillo, and W.S. Drisdell *et al.*, 2016.

## ELECTROLYTE SELECTION: CHOICE OF CATION

Use of  $\text{CsHCO}_3$  buffer increases FE to  $\text{C}_{2+}$  products (ethanol, ethylene) on Cu foil



-1.0 V vs RHE in  $\text{CO}_2$ -saturated 0.1 M  $\text{MHCO}_3$

Singh, M. R.; Kwon, Y.; Lum, Y.; Ager, J. W.; Bell, A. T.  
*J. Am. Chem. Soc.* **2016**, 138, 13006–13012.

Also: Murata, A.; Hori, Y. *Bull. Chem. Soc. Jpn.* **1991**, 64, 123–127.

# IDENTIFICATION OF ELECTROCATALYSTS FOR CO<sub>2</sub>RR TO H<sub>2</sub>COO

## Scientific Achievement

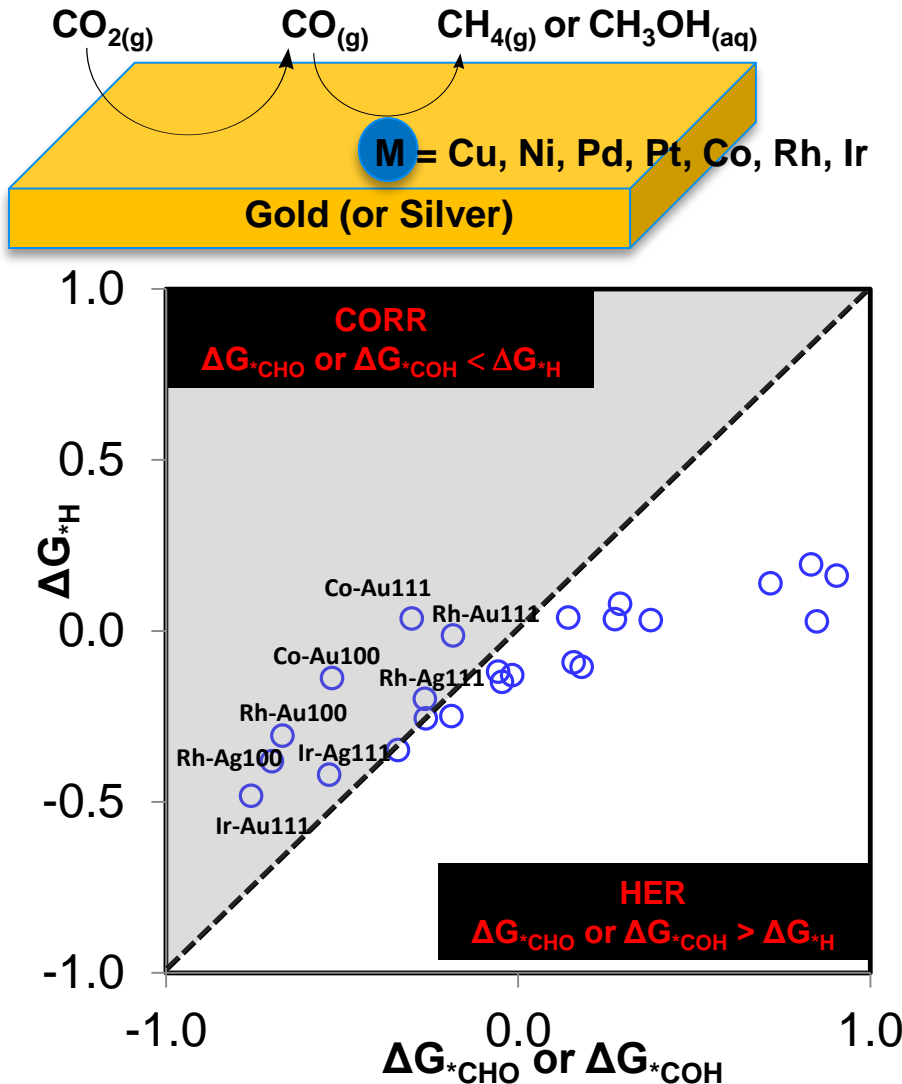
Identified tandem, bimetallic catalysts for the preferential formation of H<sub>2</sub>COO over H<sub>2</sub>.

## Significance and Impact

Selective reduction of CO<sub>2</sub> to H<sub>2</sub>COO can be achieved by embedding metal atoms that favor CORR over HER in a host metal that favors CO<sub>2</sub> reduction to CO. The CORR catalyst must bind \*CHO (or \*COH) more tightly than \*H

## Research Details

DFT/RPBE/APW was used to calculate the free energy of activation for all elementary steps in CO<sub>2</sub> reduction to CO on Au(111) or Ag(111) surfaces and the reduction of CO to H<sub>2</sub>CO vs H<sub>2</sub> on Cu, Ni, Pd, Pt, Co, Rh, and Ir atoms embedded in the host metal surface.



## ELECTROCHEMICAL REDUCTION OF CO<sub>2</sub> SELECTIVELY TO METHANOL

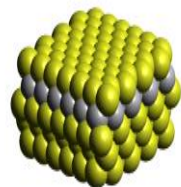
### Near-Surface Alloy for Selective Reduction of CO<sub>2</sub> to CH<sub>3</sub>OH

A theoretical prediction: a near-surface alloy (NSA) of a monolayer of Au on bulk W was empirically found to generate CH<sub>3</sub>OH to the *exclusion* of other hydrocarbons and alcohols.

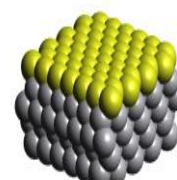
### Approach

- Combined density-functional theory and adsorption-energy descriptors  $\Delta G^\circ_{\text{CO}}$ ,  $\Delta G^\circ_{\text{H}}$  and  $\Delta G^\circ_{\text{OH}}$  predicted a Au-W-Au NSA that would be CH<sub>3</sub>OH-product-selective.
- Overlayer NSA films of (0.5 to 3 ML) Au on W were prepared by controlled galvanostatic deposition.

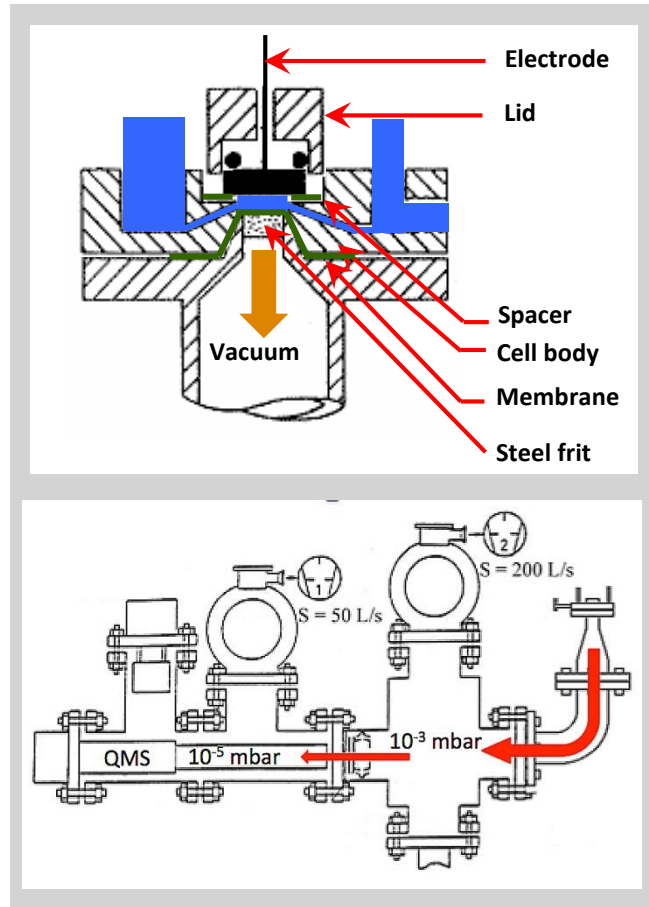
Theoretical Model  
Au-W on Au



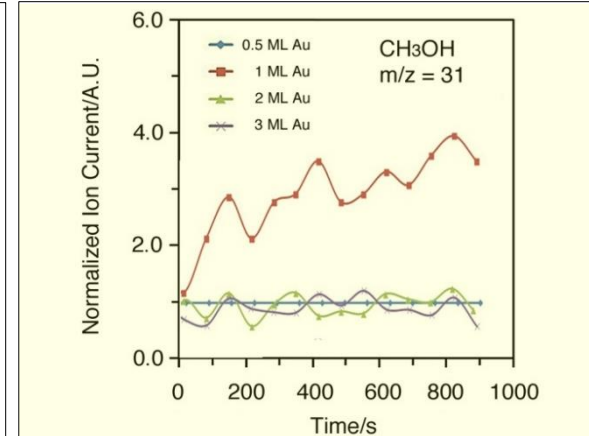
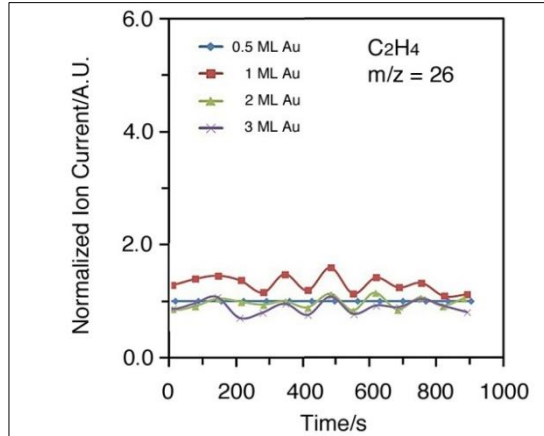
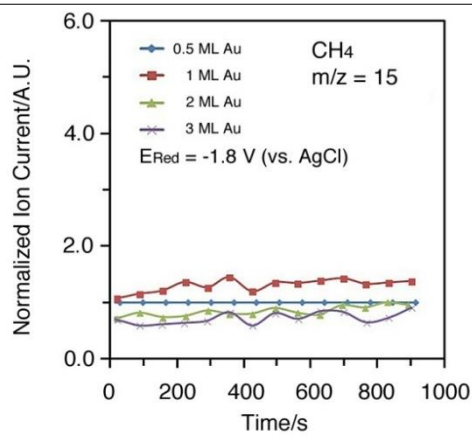
Experimental Mimic  
Au on W



[Back, et al., "Selective CO<sub>2</sub> Electroreduction to Methanol." ACS Catal. 2015, 5, 965.](#)



Products from CO<sub>2</sub> reduction at -1.2 V(RHE) in 0.1 M KHCO<sub>3</sub> were analyzed by Differential Electrochemical Mass Spectrometry (DEMS). Only CH<sub>3</sub>OH was found.

ELECTROCHEMICAL REDUCTION OF CO<sub>2</sub> SELECTIVELY TO METHANOLConstant-potential DEMS of CO<sub>2</sub> Reduction on Au-W Near-Surface Alloy**Theoretical Prognosis**

CH<sub>3</sub>OH-Selective  
High Activity  
Low Overvoltage  
HER Suppression

**Experimental Result**

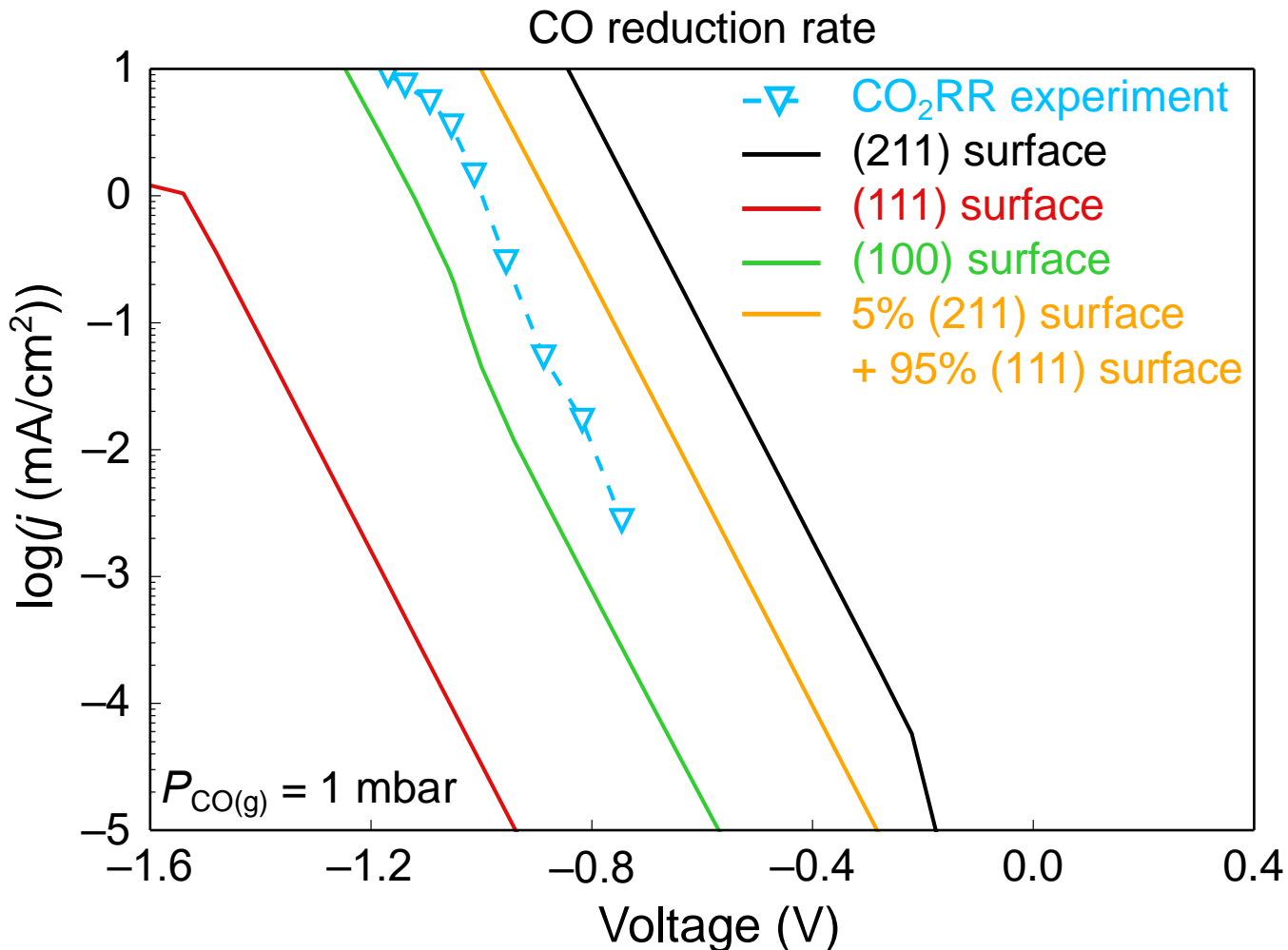
CH<sub>3</sub>OH-Selective  
Not yet optimized  
Not yet optimized  
Not yet optimized

**Future Work:**

Prepare NSA as prescribed by theory  
Try different substrates with the same NSA  
Obtain complete and quantitative product analysis  
Have theory scrutinized by other theory groups

A. Javier, J. H. Baricuatro, Y.-G. Kim and M. P. Soriaga\*. "Au-on-W Near-Surface Alloy as a CH<sub>3</sub>OH-Product-Selective Electrocatalyst for CO<sub>2</sub> Reduction: Empirical (DEMS) Confirmation of a Computational (DFT) Prediction." *Electrocatalysis*, **6** 495. (2015).

## POLARIZATION CURVES, Cu – THEORY VS EXPERIMENT



Liu, Xiao, Peng, Hong, Chan, Nørskov, Nature Comm. (2017)

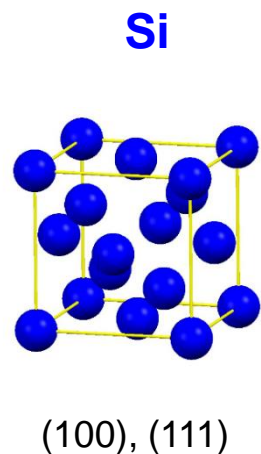
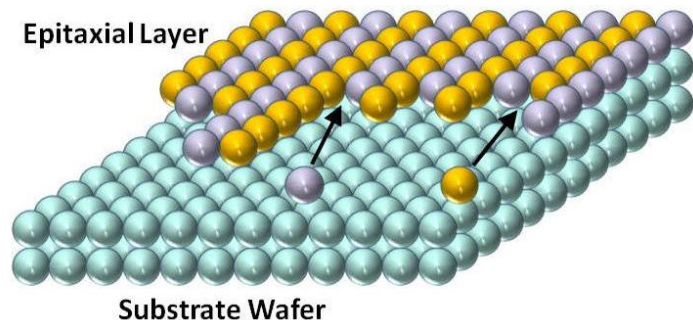
Exp.: Kuhl, et al. JACS doi:10.1021/ja505791r (2014).

Kuhl, Cave, Abram, Jaramillo,

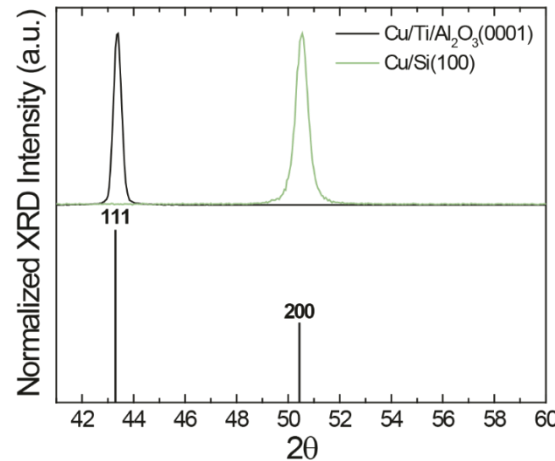
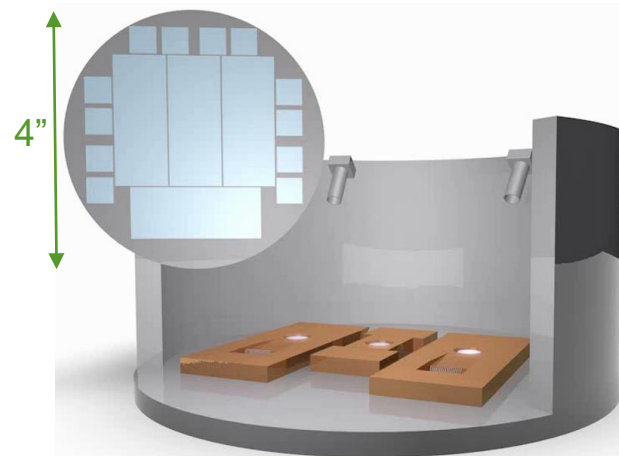
Energy & Environmental Science 5, 7050 (2012).

# EPITAXIAL GROWTH USING PHYSICAL VAPOR DEPOSITION

Directing growth orientation utilizing interfacial energy



E-beam Evaporation

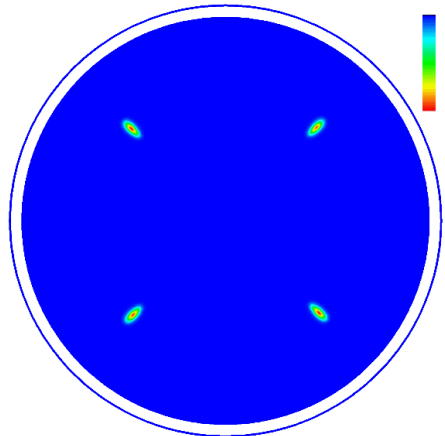
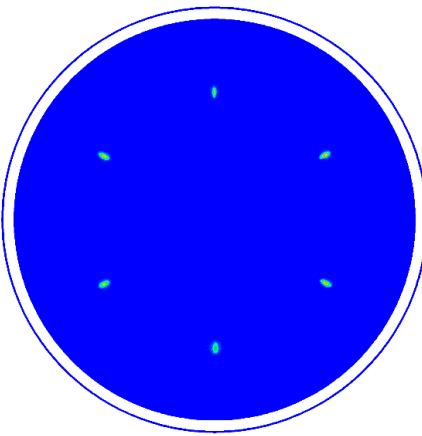
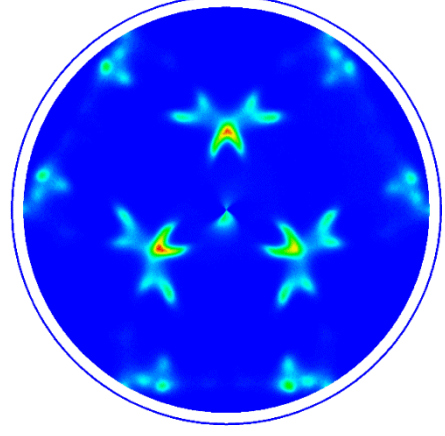


D. B. Knorr and T.-M. Lu, *Textures and Microstructures*, **1991**, 13, 155-164.

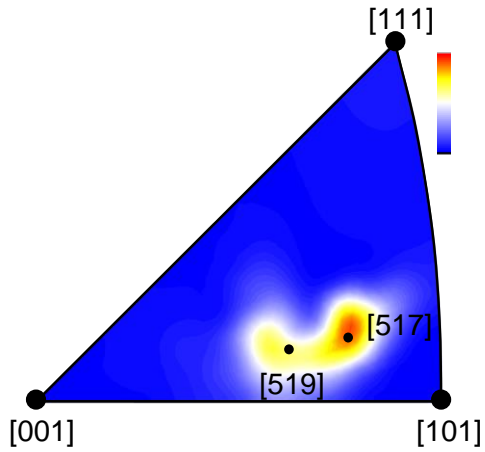
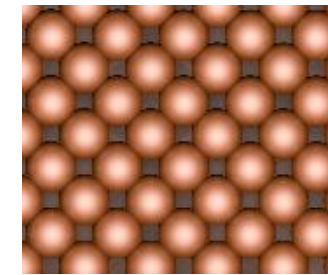
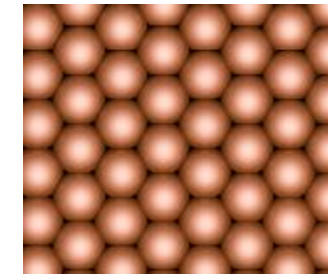
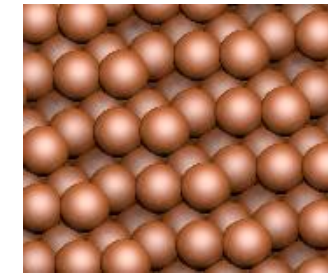
B. G. Demczyk, R. Naik, G. Auner, C. Kota and U. Rao, *Journal of Applied Physics*, **1994**, 75, 1956-1961.

I. Hashim, B. Park, and H.A. Atwater, *Applied Physics Letters*, **1993**, 63, 2833-2835.

## TEXTURE OF Cu THIN FILMS

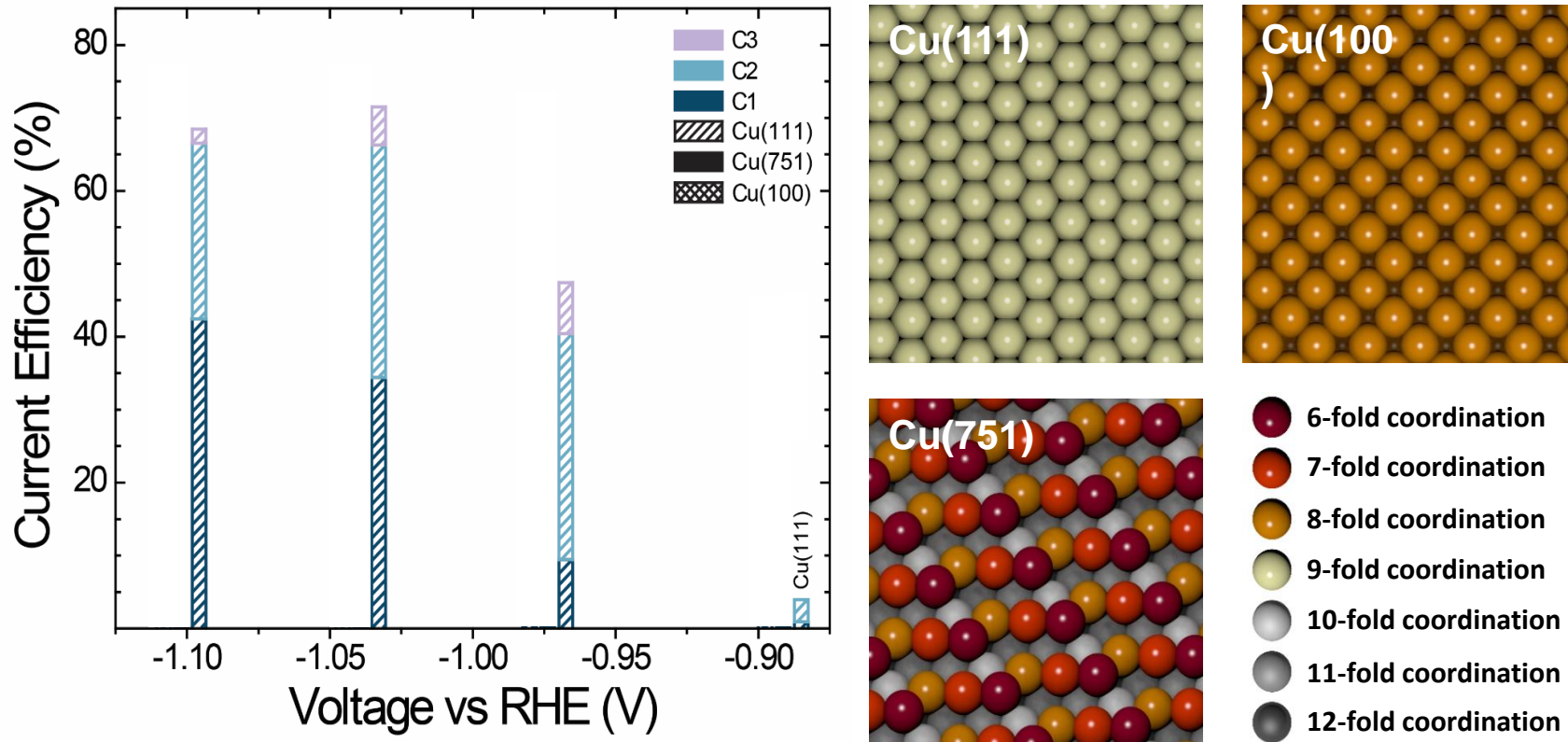
 $\text{Cu}(100)/\text{Si}(100)$  $\text{Cu}(111)/\text{Al}_2\text{O}_3(0001)$  $\text{Cu}(751)/\text{Si}(111)$ 

Inverse Pole Figure

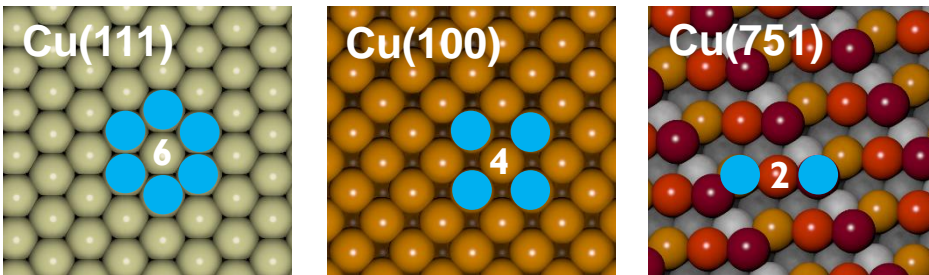
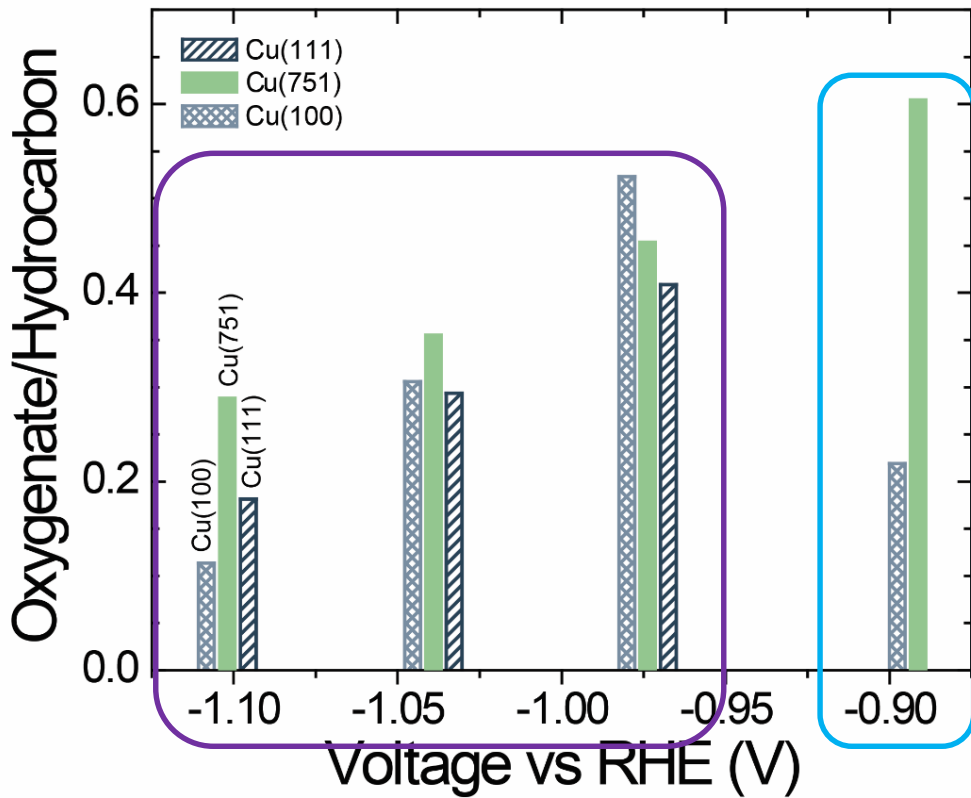
 $\text{Cu}(100)$  $\text{Cu}(111)$  $\text{Cu}(751)$ 

C. Hahn, T. Hatsukade, Y.G. Kim, A. Vallionis, J.H. Baricuatro, D.C. Higgins, S. Nitopi, M.P. Soriaga and T.F. Jaramillo, PNAS, 2017.

## EFFECTS OF SURFACE STRUCTURE ON C-C COUPLING SELECTIVITY

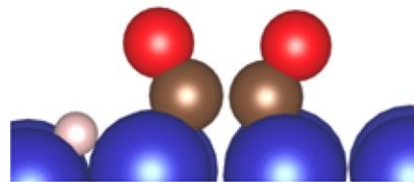


C-C coupling is favored on under-coordinated sites.  
Epitaxial Cu thin films are single-crystal analogous for C-C coupling selectivity.



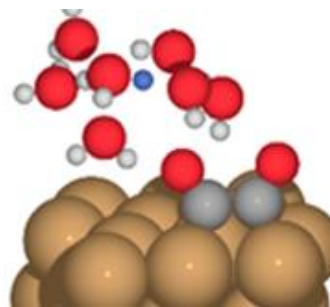
Cu(751) has the lowest number of nearest neighbors, and is the least likely to have adsorbed H\* adjacent to C2 intermediates.  
 PCET instead of hydride transfer leads to less structure sensitivity.

## Hydride Transfer



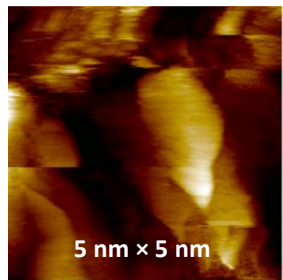
J.D. Goodpaster, A.T. Bell, M. Head-Gordon,  
*JCPL*, 2016, 7, 1471-1477.

## Proton-coupled Electron Transfer

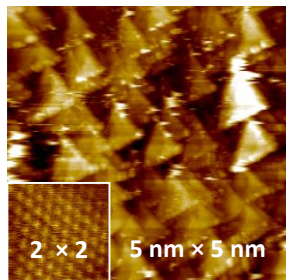


# STRATEGIES FOR SELECTIVE CO<sub>2</sub> REDUCTION REACTIONS

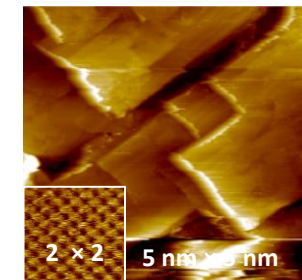
## OECSTM: Cu RECONSTRUCTION AT CO<sub>2</sub>R CONDITIONS (-0.9 V/0.1 M KOH)



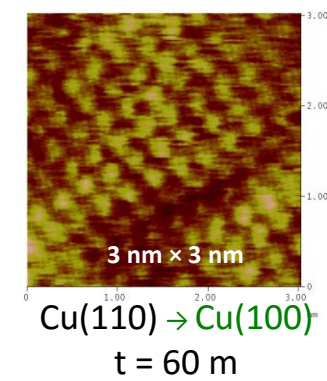
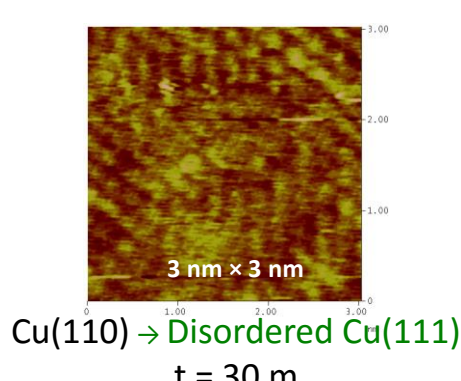
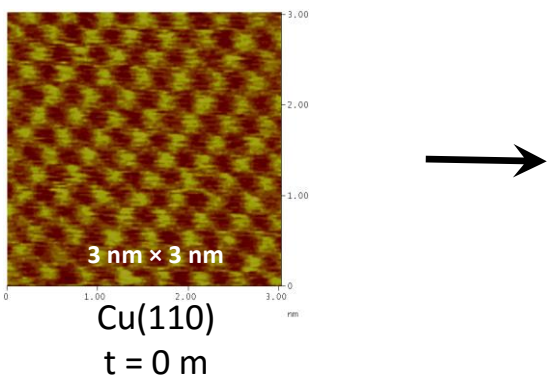
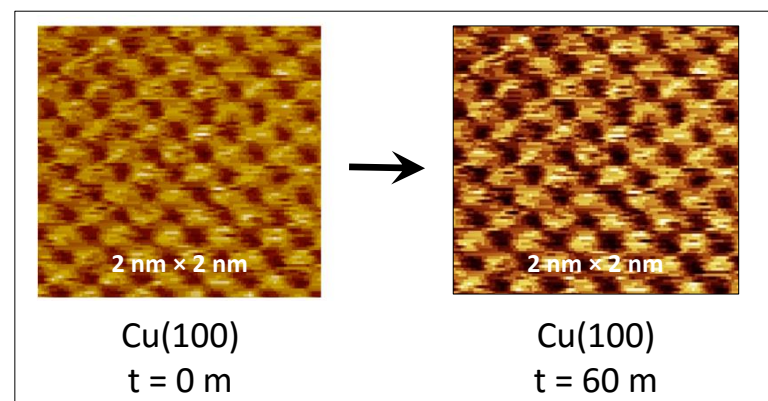
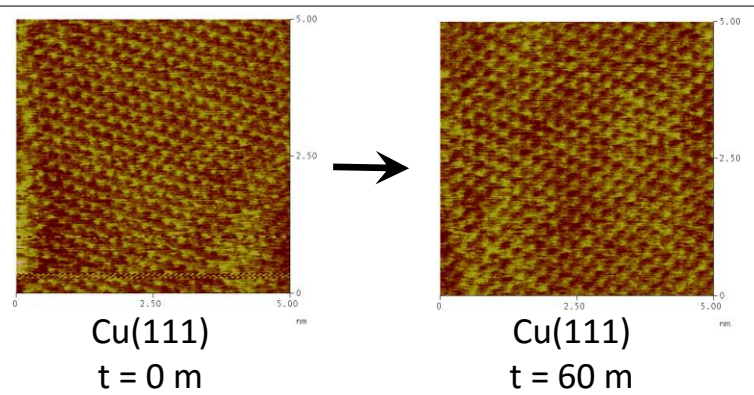
Cu(pc)  
t = 0 m



Cu(pc) → Cu(111)  
t = 30 m



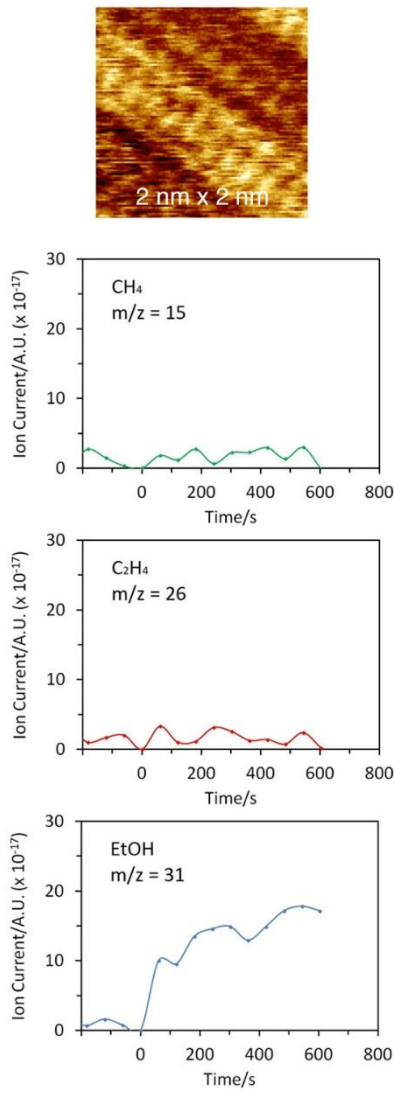
Cu(pc) → Cu(111) → Cu(100)  
t = 60 m



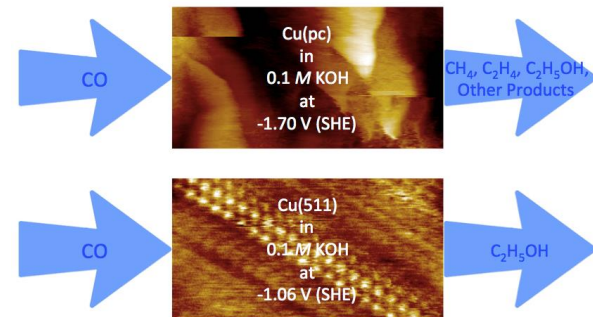
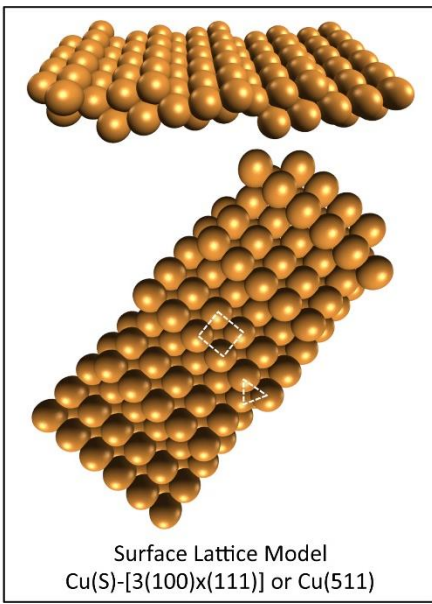
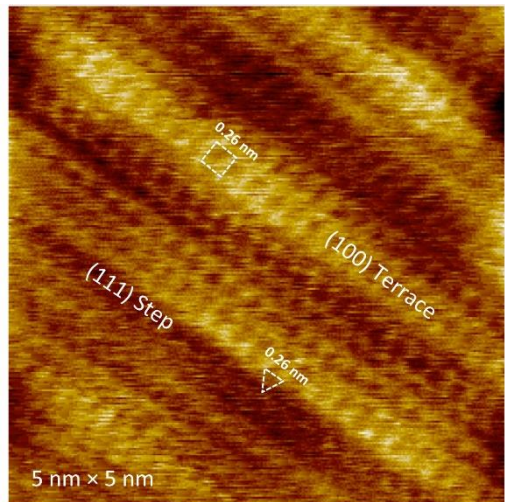
# STRATEGIES FOR SELECTIVE CO<sub>2</sub> REDUCTION REACTIONS

## REGULATING CO-REDUCTION SELECTIVITY BY CONTROL OF SURFACE STRUCTURE

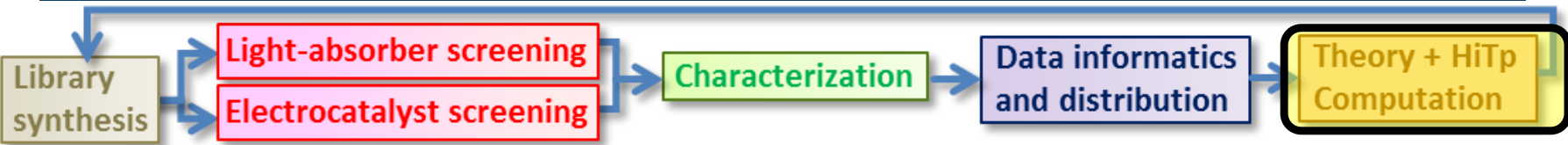
Ethanol-product Selectivity of Post-ORC Cu(pc)-[Cu(100)] at -1.0 V in 0.1 M KOH



CO-to-C<sub>2</sub>H<sub>5</sub>OH on Cu(511)

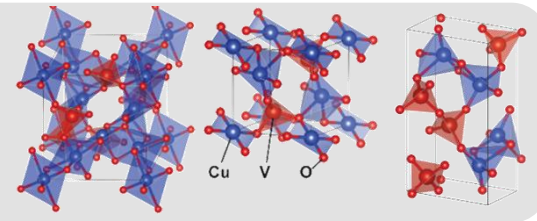


## HIGH THROUGHPUT DISCOVERY OF PHOTONODES



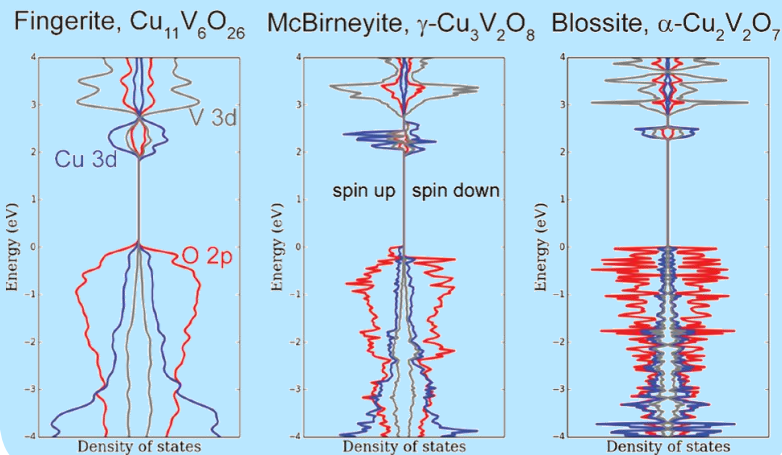
### Design Materials & Interface with MP Database

Joint project with the Materials Project to design photoanodes and identify candidate materials.



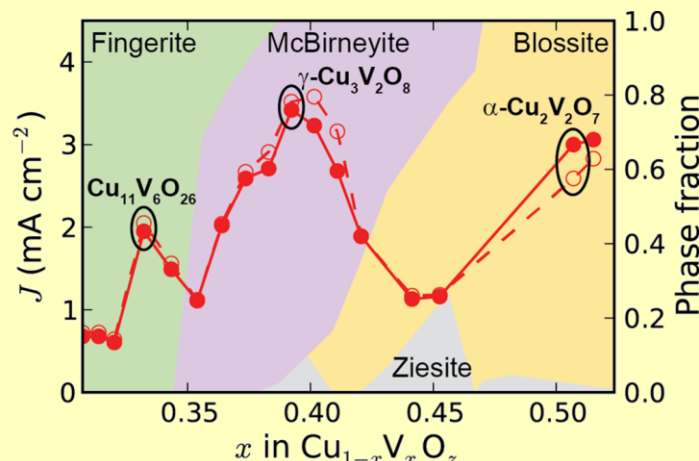
### High Throughput Computation

Judicious choice of functional to rapidly evaluate the electronic structure and Pourbaix stability of hundreds of materials



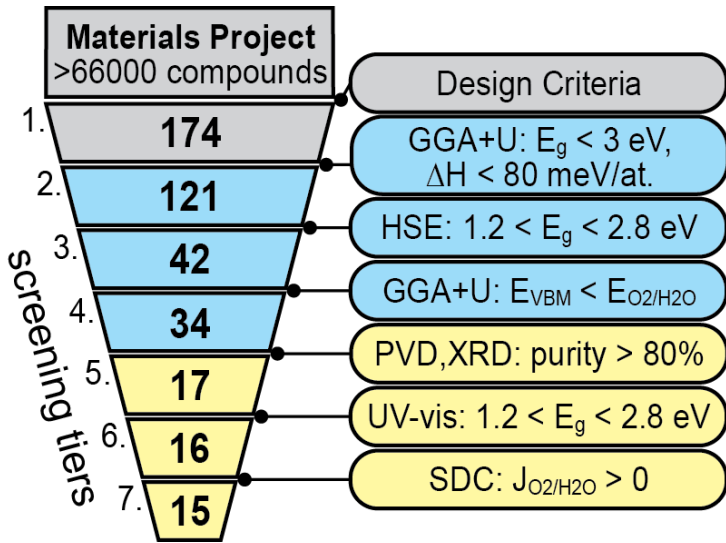
### High Throughput Experimentation

Identify synthesis conditions, generate composition maps of optical and photoelectrochemical properties.



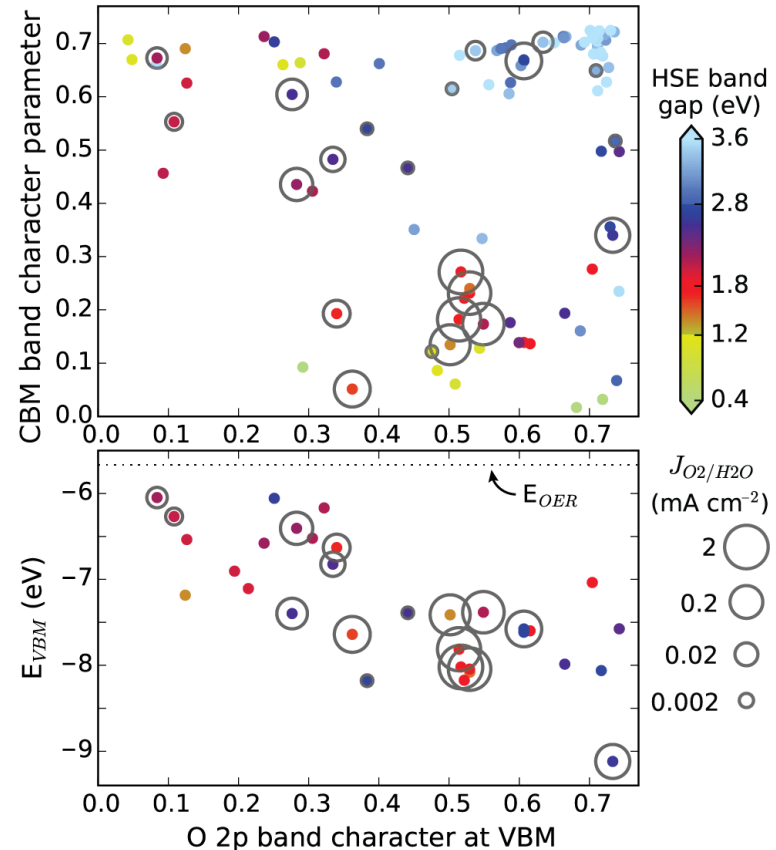
# HIGH THROUGHPUT DISCOVERY OF PHOTOANODES: INTEGRATED THEORY-EXPERIMENT PIPELINE

Stitching complementary techniques together accelerates hypothesis-based discoveries



## Pipeline execution summary:

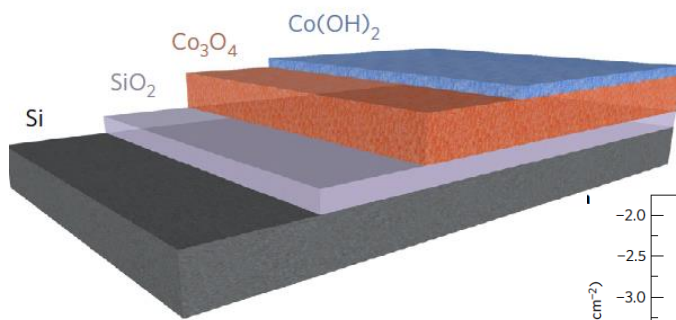
- Out of the 15 hits there are 12 discoveries (3 of 15 were already reported)
- The 88% hit rate upon successful synthesis provides credence to the design criteria and the computational workflow
- These experimentally-verified predictions foundationally demonstrate that high throughput computation can accelerate experimental discovery of functional materials.



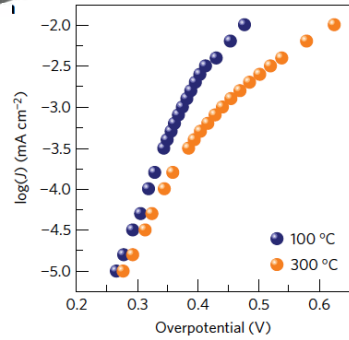
- Varying the electronic band character in complex oxides enables tuning of the band gap energy and band positions.

Q. Yan, et.al. (Persson, Gregoire, Neaton) PNAS, 114 3040-3043 (2017).

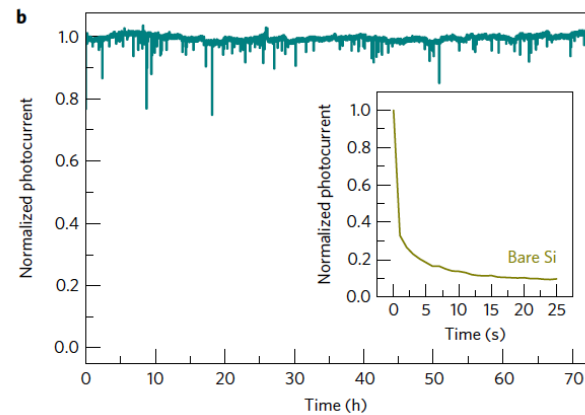
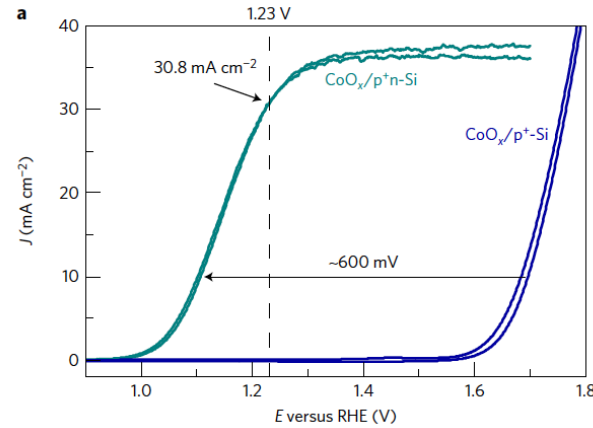
## BIPHASIC OER CATALYST INTEGRATED ON Si



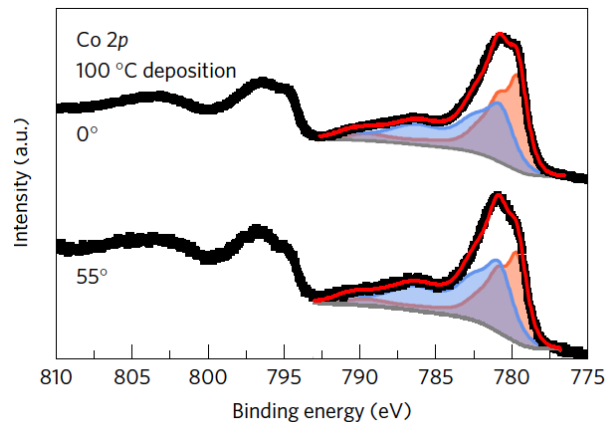
Tafel slope:  
~50mV/decade:



Onset potential for water oxidation of <1V versus RHE  
and a saturation current density of 37.5 mA/cm<sup>2</sup>:

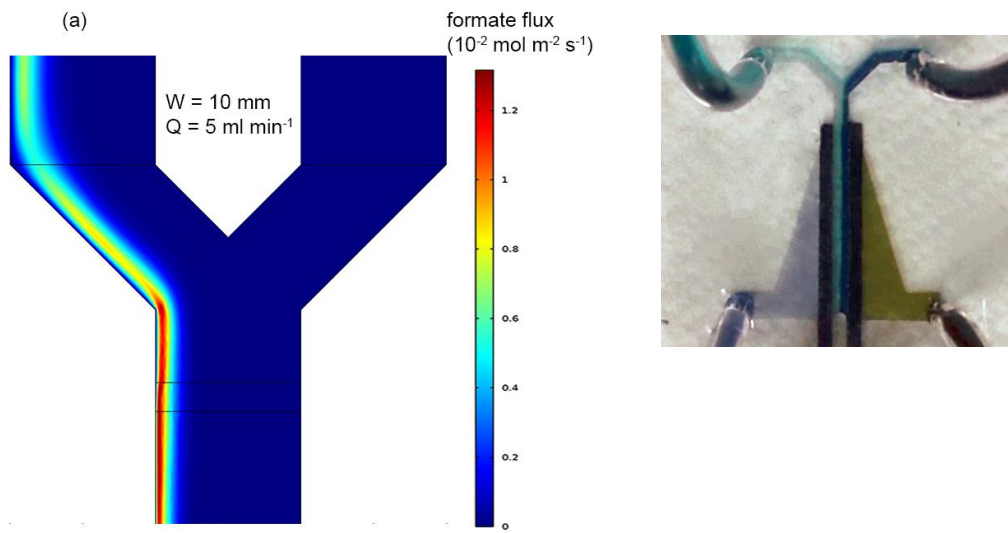


More Co(OH)<sub>2</sub> component increases with increasing photoelectron take-off angle → surface layer:



No detectable transfer of Co from the film into solution after 72 hr.

## MEMBRANELESS FLOW CELL PROTOTYPE FOR SEPARATIONS

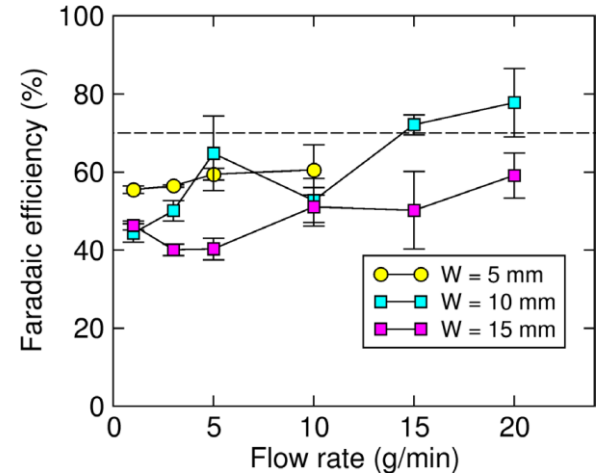


**A new electrochemical  $\text{CO}_2$  test bed implements isolates the fuel-containing electrolyte produced at the cathode from the anode and produces a stream of liquid products.**

Cell design validated with 2-D Multiphysics modeling and experimentally implemented.

Separation efficiency as high as 90% demonstrated.

Monroe, M. M.; Lobaccaro, P.; Lum, Y.; Ager, J. W., *J. Phys. D. Appl. Phys.* 50, 154006 (2017).

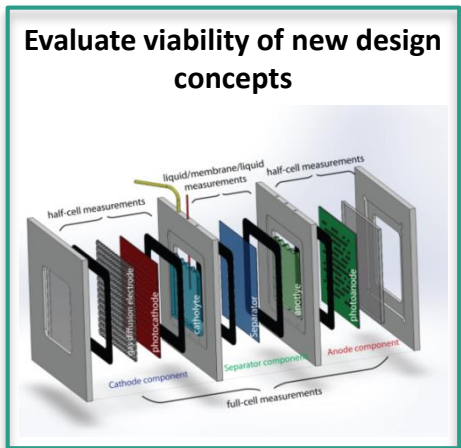
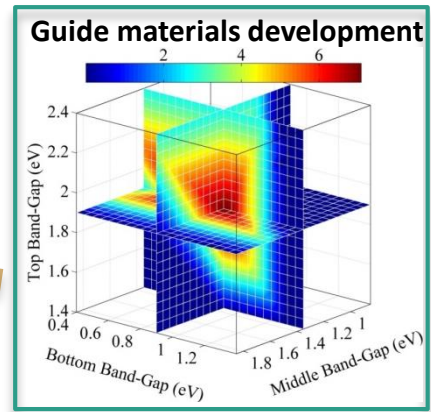
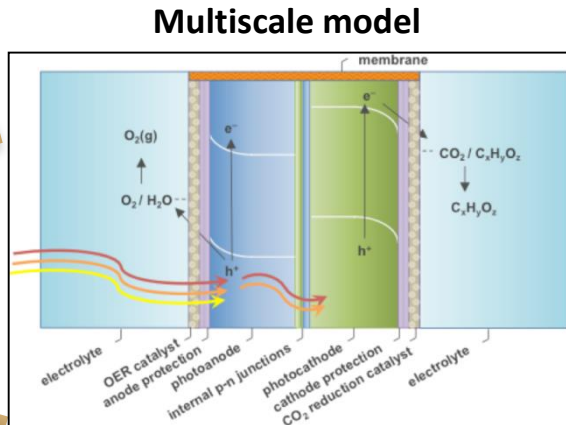
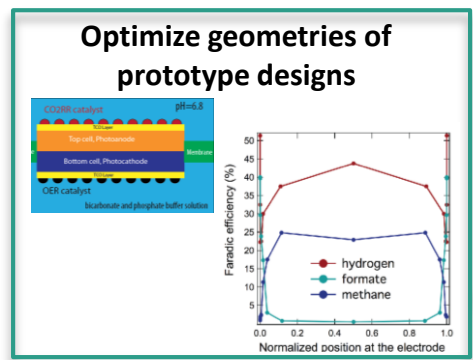


Overall Faradaic efficiency (sum of both channels) for formate production with 0.1 M  $\text{KHCO}_3$  electrolyte saturated in  $\text{CO}_2$  and Sn cathode at  $5 \text{ mA/cm}^2$ .

Goulet, M.A.; Kjeang, E. *J. of Power Sources*. 2014, 260, 186-196.

Ismagilov, R.F.; Stroock, A.D.; Kenis, P.J.A.; et al. *Appl. Phys. Letters*. 2000, 76, 2376-2378.

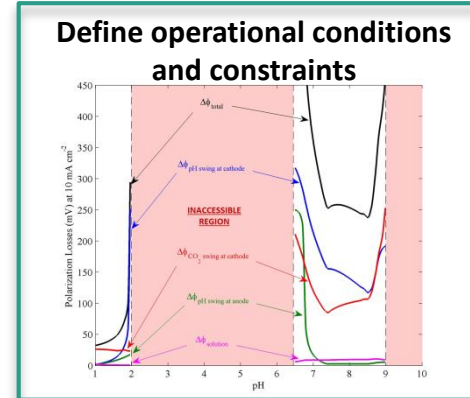
# MULTIPHYSICS MODELING: VIRTUAL INTEGRATOR AND TESTING PLATFORM



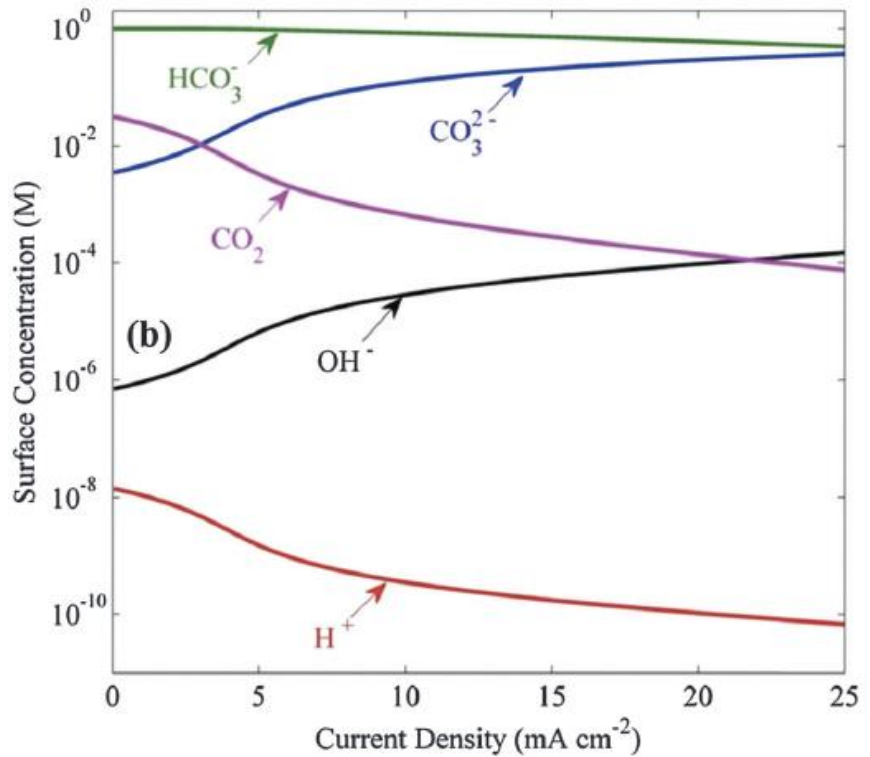
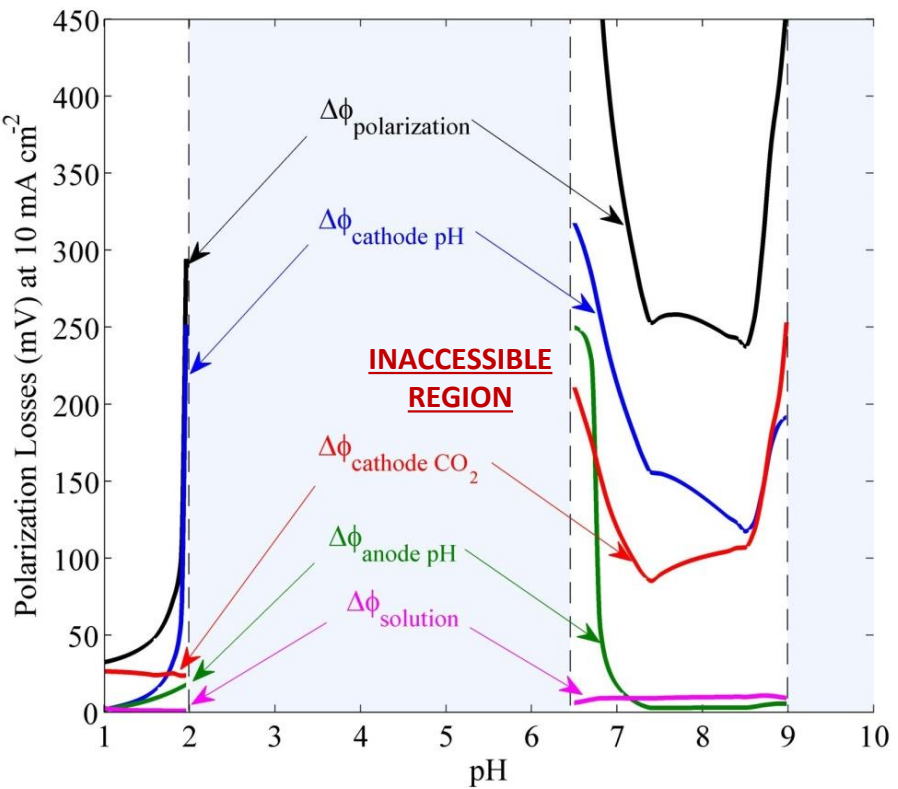
## Understand cell performance in real-life environment



	Barstow	Albuquerque	New Orleans	Quillayute
Weighted Average Annual MJ/m² [kWh]	11.2	11.0	10.0	9.1
Annual kg of H <sub>2</sub> Produced per [sq. m] of Aperture	8.80	7.98	4.85	2.91



## EXPLORING DEVICE-LEVEL LIMITATIONS



- 20  $\text{mA/cm}^2$  is feasible with 1 atm  $\text{CO}_2$  or equivalent high concentration locally
- For aqueous: pH 7.5 to 8.5 shows lowest total losses while maintaining selectivity towards  $\text{CO}_2$  reduction

Key is local  $\text{CO}_2$  concentration

- A strategy for selective EC-CO<sub>2</sub> reduction: multifunctional cathode that combines multiple active sites, functional coatings, nanoscale confining volumes
- Mechanism discovery: initial focus predominantly on Cu and Cu alloys
- Materials discovery:
  - bimetallic alloy candidates screened and synthesized
  - oxide photoanode theory/experimental effort achieves high predictive yield
- Integration - focus on OER (– biphasic cobalt oxide)
- Prototyping: device architectures for EC and PEC CO<sub>2</sub>RR



**SLAC**



